Electronic Supplementary Information

Reactant or Reagent? Oxidation of H_2 at Electronically Distinct Nickel-Thiolate Sites $[Ni_2(\mu\text{-}SR)_2]^+$ and $[Ni\text{-}SR]^+$

Felix Koch and Andreas Berkefeld*

Table of contents

1. General Information

All manipulations of air- and moisture-sensitive compounds were carried out under an atmosphere of dry argon using standard Schlenk or glove-box techniques. Compounds [**1**]NTf_2,[1] [**1**-H]NTf_2,[1] [**2**][NTf_2]$_2$,[2] [Fc]NTf_2,[1] Ni(cod)$_2$,[3] and Ni(PMe_3)$_4$[4] were prepared according to literature procedures. NTf_2 denotes the (F_3CSO_2)N-anion. N,N,N',N'-Tetrametyl-1,8-diaminonaphthalene (= base; 99%, Sigma Aldrich), sodium tris(acetoxy)borohydride (Na[HB(OAc)$_3$]; 95%, ABCR), and PMe_3 (1M in toluene, Sigma Aldrich) were used as received and stored under argon. Bis(trifluoromethanesulfonyl)amide ($HNTf_2$; 99%, Acros Organics) and cobaltocene (Cp_2Co; 99%, ABCR) were sublimed once before use. Solvents were purified and dried prior to use. Dichloromethane and hexane were dried using an MBraun solvent purification system (SPS). Diethyl ether and THF were predried over activated 3 Å molecular sieves (MS) and distilled from sodium benzophenone ketyl or potassium metal under argon. 2-Methyl-tetrahydrofuran (2-Me-THF; >99%, inhibitor free, Sigma Aldrich), d_8-THF and C_6D_6 were dried over and distilled from NaK alloy and stored in the glove box. $CDCl_3$ and CD_2Cl_2 were dried over and vacuum transferred from 3 Å MS. Acetonitrile (MeCN) for use in electrochemical experiments was sequentially dried over and distilled from CaH_2 and P_2O_5, and finally percolated through activated neutral alumina. 1,2-$C_6H_4F_2$ (ABCR) was percolated through activated neutral alumina and distilled under argon. All solvents were stored over 3 Å MS or activated neutral alumina (MeCN, 1,2-$C_6H_4F_2$) under argon. Molecular sieves and neutral alumina were activated by heating under dynamic vacuum (10^{-3} mbar) at 250°C for 24-48 h. NMR data were recorded on Bruker AVII+500, Avance II 400 and DRX 250 NMR spectrometers. δ values are given in ppm, J values in Hz. ^{1}H and ^{13}C{^{1}H} NMR chemical shifts are referenced to the residual ^{1}H and natural abundance ^{13}C resonances of the solvents: δ = 7.16/128.06 (C_6D_6), 1.72/67.21 (C_4D_8O), 5.32/53.84

(CD_2Cl_2) and 7.26/77.16 ($CDCl_3$). ^{31}P NMR chemical shifts are referenced to external standard sample of 85% H_3PO_4 set to δ_P = 0 ppm. Electronic spectra were recorded with a PerkinElmer Lambda 35 UV/vis photospectrometer equipped with a Unisoku CoolSpeK UV USP-203-B cryostat, using a gas tight, four-side-transparent fused 1 cm quartz cuvette fused with a 25 mL flask (cf. Figure S20). Cyclic voltammetric (CV) studies were carried out at controlled temperature (thermostat set to 24°C) under an argon atmosphere using an ECi 200 potentiostat (Nordic Electrochemistry) in a gas-tight, full-glass, three-electrode cell setup. nBu_4NPF_6 electrolyte (Alfa Aesar) was recrystallized 3 times from acetone/water, dried unter dynamic vacuum at 150°C, and employed as a 0.1 M solution in 1,2-$C_6H_4F_2$ and MeCN. $AgClO_4$ (anhydrous, Alfa Aesar) was used as received. The potentiostat was controlled using the EC4 DAQ (version 4.1.90.1, Nordic Electrochemistry) software, and data were treated with EC4 VIEW (version 1.2.36.1, Nordic Electrochemistry). A glassy carbon disc (Metrohm, electro-active area = 0.08 ± 0.002 cm^2) and a 1 mm coiled Pt-wire were employed as working and counter electrodes, respectively. A 0.5 mm Ag wire in a 0.01 M $AgClO_4$/ 0.1 M nBu_4NPF_6 MeCN solution served as a reference electrode. IR compensation was applied during data collection, and CV data were corrected for background currents of electrolyte solutions for different potential sweep rates. Potentials are reported relative to E^0(Fc/$[Fc]^+$, 0.1 M nBu_4NPF_6/1,2-$C_6H_4F_2$, 24°C) = 0.222 ± 0.003 V vs Ag/Ag^+. The electroactive area of the working electrode was calculated from Fc/$[Fc]^+$ measurements in 0.1 M nBu_4NPF_6 solution in MeCN at various concentrations and potential sweep rates, using D(Fc/MeCN, 20°C) = 2.40×10^{-5} cm^2 s^{-1}. The working electrode was rinsed with acetone, polished very gently with a paste of 0.3 μm alumina (Metrohm) in deionized water, rinsed thoroughly with plenty of deionized water, and finally acetone after each use and stored in a desiccator over P_2O_5. Periodic Fc/$[Fc]^+$ reference measurements verify the integrity of the working

electrode as well as the stability of the Ag/Ag^+ reference potential. X-band cw-EPR spectra were collected using 4 mm O.D. Wilmad quartz (CFQ) sample tubes on a Bruker ESP 300E cw-spectrometer, and are referenced to the Bruker Strong Pitch standard g_{iso} = 2.0028. EasySpin[5] (version 5.0.21) implemented in MATLAB (Statistic Toolbox Release R2016a, The MathWOrks, Inc., Natick, Massachusetts, United States) was used for digital simulation of EPR data. Spectral fitting was carried out using the easyfit tool included in EasySpin package, using either pepper for solid state or garlic for solution EPR data.

2. Supplementary NMR Spectroscopic Data

General remark. Complexes [**1**]NTf_2 and [**2**][NTf_2]$_2$ were used as crystalline starting materials in reactions discussed in this work. Compound [**2**][NTf_2]$_2$ is subject to a slow loss of Ni(NTf_2)$_2$ in donor solvents like THF which affords mononuclear **3**[6] (Figure S1). Characteristic resonances owing to the formation of **3** are highlighted by **$** in the following.

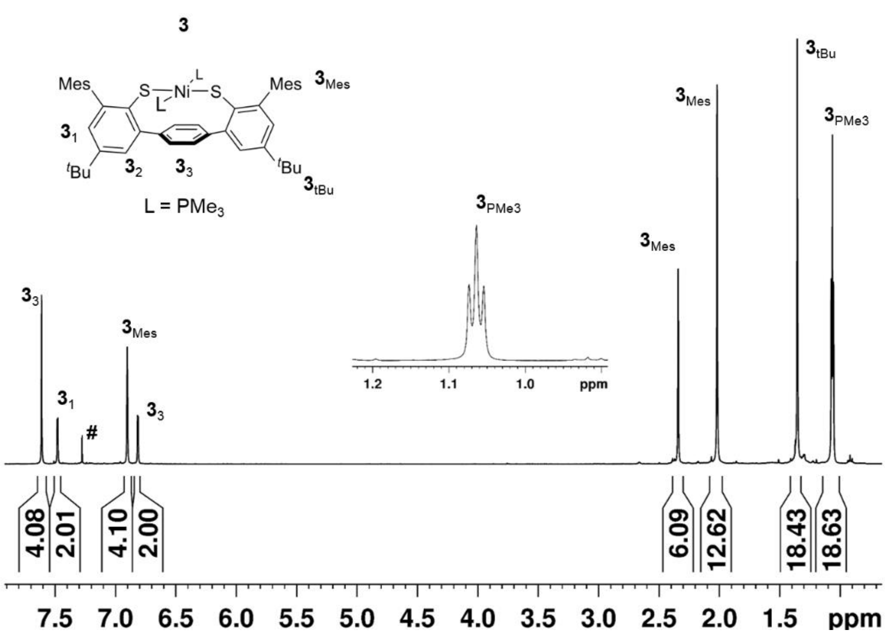

Figure S1. ^{1}H NMR spectrum (400 MHz, $CDCl_3$ (#), 26°C): Representative spectrum of complex **3**; *Inset*: characteristic *N*-line pattern of *trans*-Ni(PMe_3)$_2$.[6]

Treatment of [1]NTf$_2$ with H$_2$ in d$_8$-THF solution.

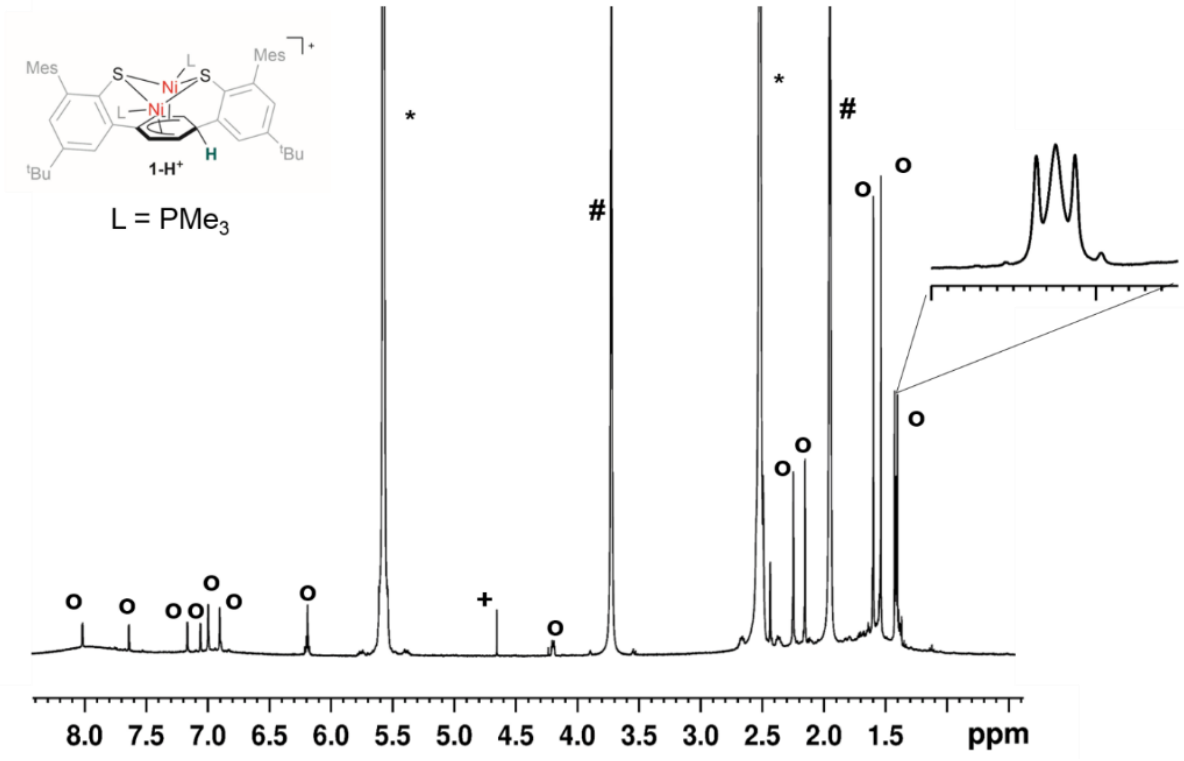

Figure S2. ^{1}H NMR spectrum (250 MHz, d$_8$-THF (#), 26°C): Reaction mixture from [**1**]$^+$ (broad resonances) exposed to 1 atm of H$_2$ (+) after 5 days at r.t., product [**1**-H]$^+$ (**O**), 1,5-cycloocadiene (*, internal standard); *Inset*: characteristic *N*-line pattern of *trans*-Ni(PMe$_3$)$_2$ of [**1**-H]$^+$.[1]

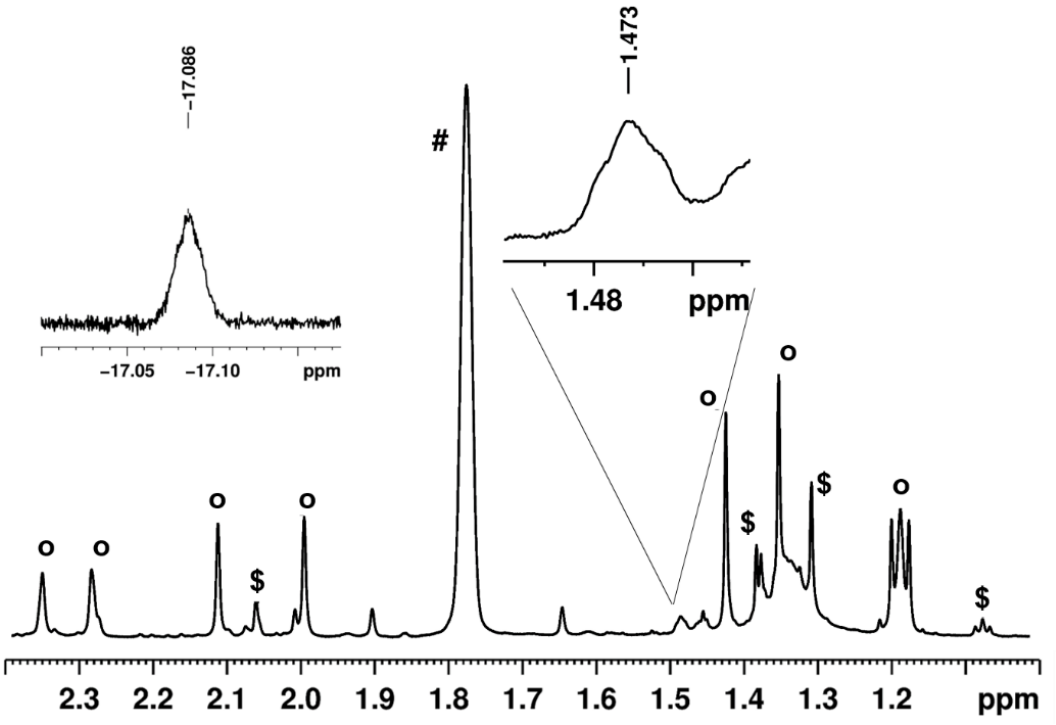

Figure S3. ^{1}H NMR spectrum (500 MHz, d_8-THF (#), 26°C): Mixture of products from [**1**]$^{+}$ under 1 atm of H_2 after 30 days at r.t., product [**1**-H]$^{+}$ (**O**), 1,5-cycloocadiene (*, internal standard); *Inset*: characteristic *N*-line pattern owing to *trans*-Ni(PMe_3)$_2$ and Ni-H of [HNi(PMe_3)$_4$]$^{+}$ at 1.47 and −17.1 ppm, respectively; **$** = co-product **3**.

Treatment of [1]NTf$_2$ with H$_2$ in propylene carbonate solution. A solution of [**1**]NTf$_2$ (10 mg, 0.084 mmol) in propylene carbonate (0.5 mL) and 50 mg C_6D_6 was placed in an NMR tube. The solution was degassed by three freeze-pump-thaw cycles and exposed to 1 atm of H_2. After 7 days at r.t., complete conversion of [**1**]$^+$ and formation of [**1**-H]$^+$ was evident from ^{1}H and ^{31}P{^{1}H} NMR spectra.[1]

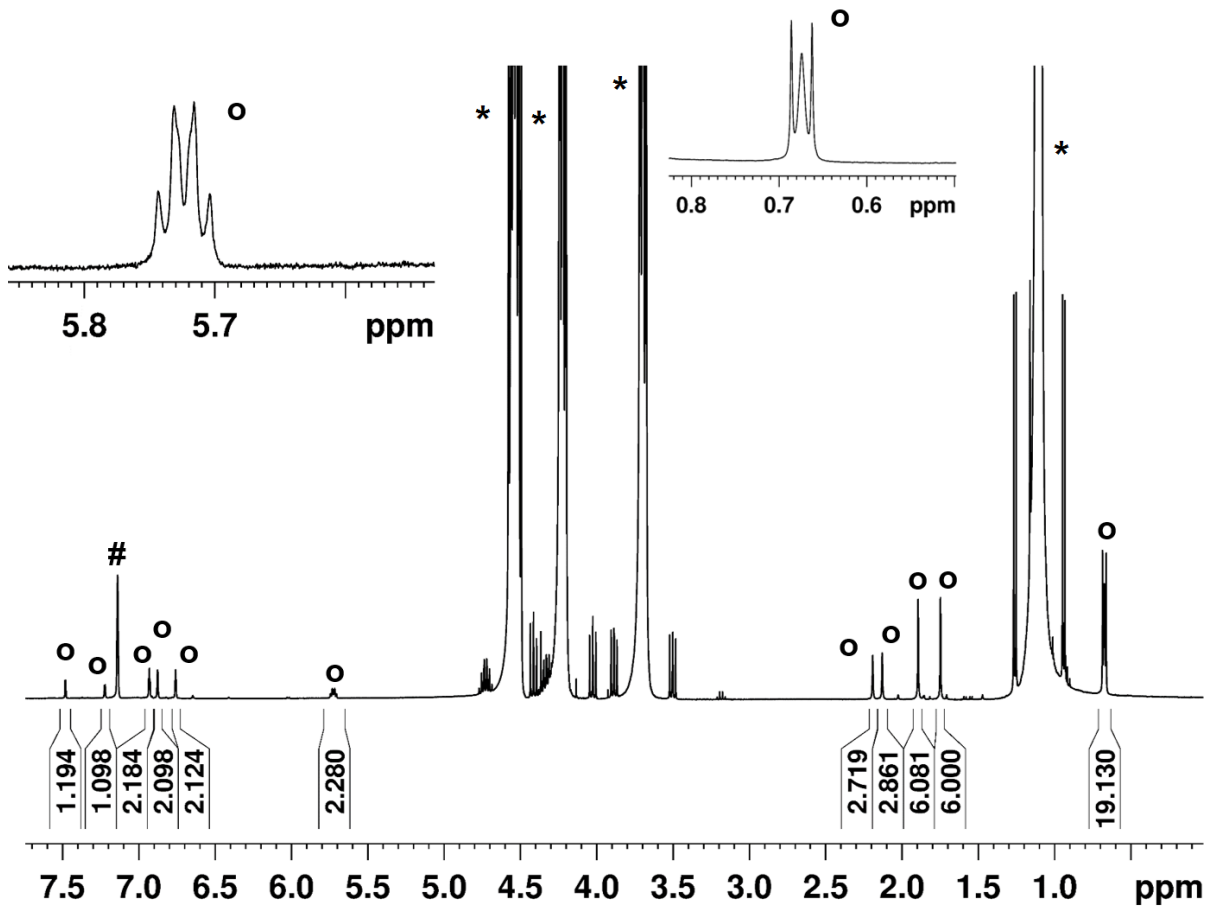

Figure S4. ^{1}H NMR spectrum (400 MHz, C_6D_6 (#), propylene carbonate (*), 26°C): Reaction mixture from [**1**]$^+$ under 1 atm of H_2 after 7 days at r.t., [**1**-H]$^+$ (**O**, product); *Insets*: characteristic resonances of μ-η^2:η^2-cyclohexadienide moiety (*left*) and *trans*-Ni(PMe$_3$)$_2$ (*right*) of [**1**-H]$^+$.[1]

Treatment of [1]NTf$_2$ with Ni(PMe$_3$)$_4$.

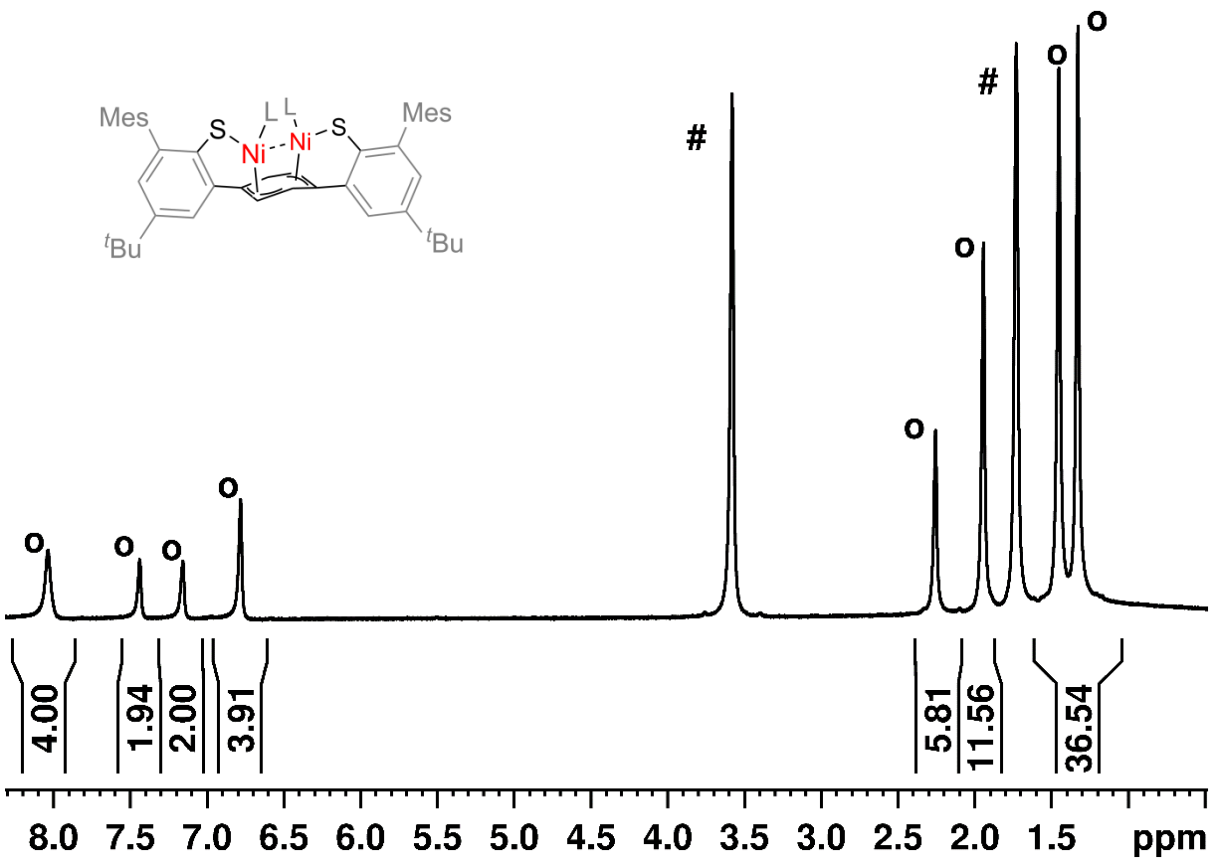

Figure S5. ^{1}H NMR spectrum (400 MHz, d$_8$-THF (#), 26°C): Reaction mixture from [**1**]$^+$ (16 mg, 0.013 mmol) and Ni(PMe$_3$)$_4$ (5 mg, 0.014 mmol) in d$_8$-THF (#, 0.5 mL) at r.t.; Signals found for **1** (**O**) match those reported previously.[6]

Treatment of [2](NTf$_2$)$_2$ with Ni(PMe$_3$)$_4$.

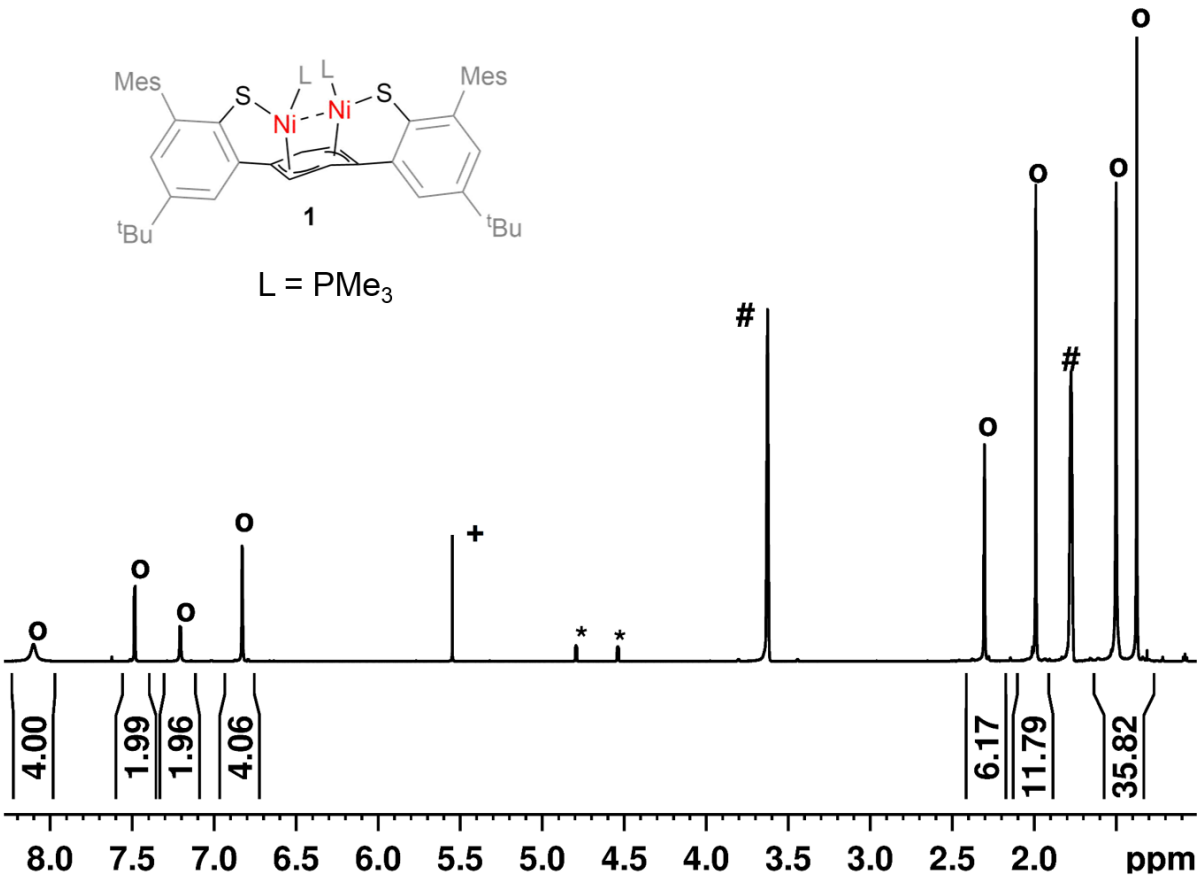

Figure S6. ^{1}H NMR spectrum (400 MHz, d$_8$-THF (#), 26°C): Reaction mixture from [**2**]$^{2+}$ (10 mg, 0.0068 mmol) and Ni(PMe$_3$)$_4$ (5 mg, 0.014 mmol) in d$_8$-THF (#, 0.5 mL) at r.t.; Signals found for **1** (**O**) match those reported previously,[6] residual CH_2Cl_2 (+), and (η^5-MeC(O)C$_4$H$_4$)$_2$Fe (*) derive from synthesis of [**2**](NTf$_2$)$_2$.

Treatment of [2](NTf$_2$)$_2$ with Ni(PMe$_3$)$_4$.

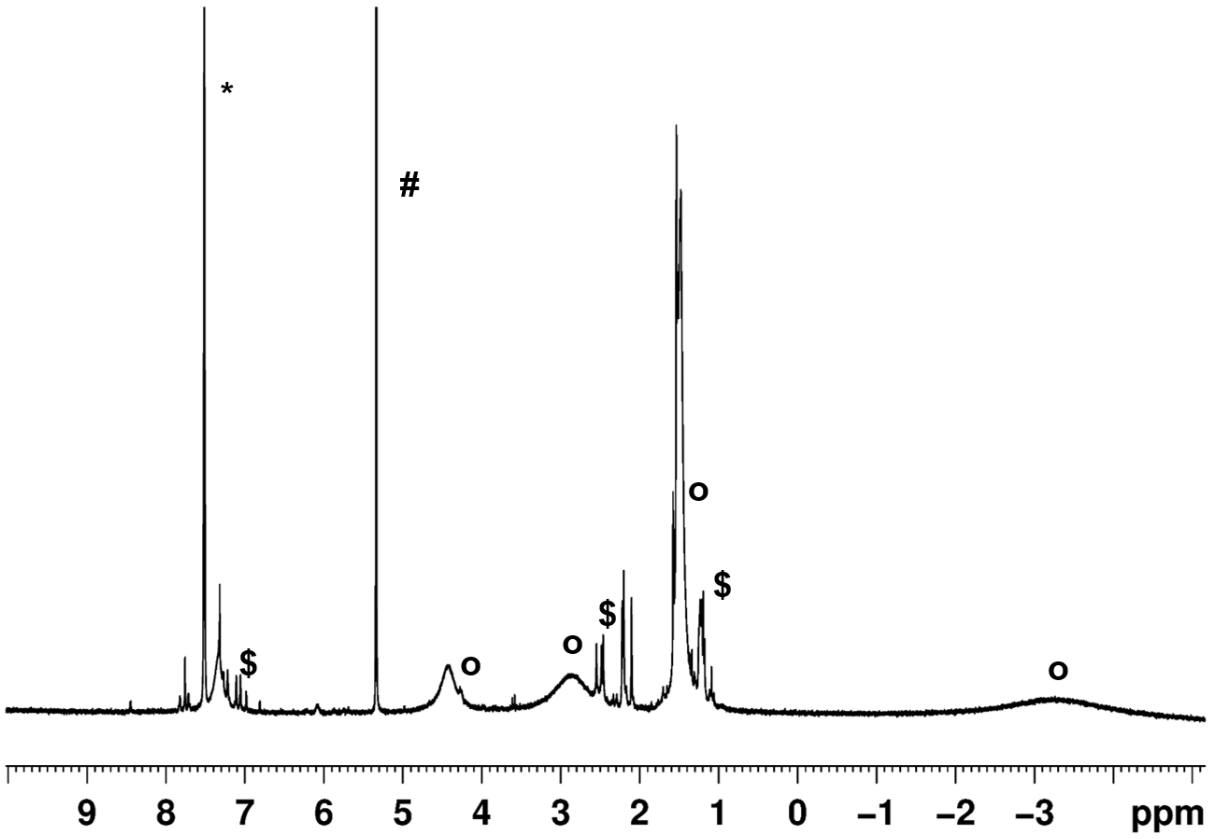

Figure S7. ^{1}H NMR spectrum (400 MHz, CD_2Cl_2 (#), 26°C): Reaction mixture from [**2**]$^{2+}$ (10 mg, 0.0068 mmol) in CD_2Cl_2 (0.5 mL) and Ni(PMe$_3$)$_4$ (2.5 mg, 0.0068 mmol) in C_6D_6 (*, 100 mg) at r.t.; Resonances of paramagnetic [**1**]$^+$ (**O**) match those reported previously,[1] **$** = decomposition product **3**.

Treament of $Ni(PMe_3)_4$ with H_2. A solution of $Ni(PMe_3)_4$ (17 mg, 0.046 mmol) and base (10 mg, 0.046 mmol) in d_8-THF (#, 0.5 mL) was placed in an NMR tube. The solution was degassed by three freeze-pump-thaw cycles and exposed to 1 atm of H_2. All resonances in ^1H and $^{31}P\{^1H\}$ NMR spectra arise from starting materials and no visual colour change was observed over a period of 1 day.

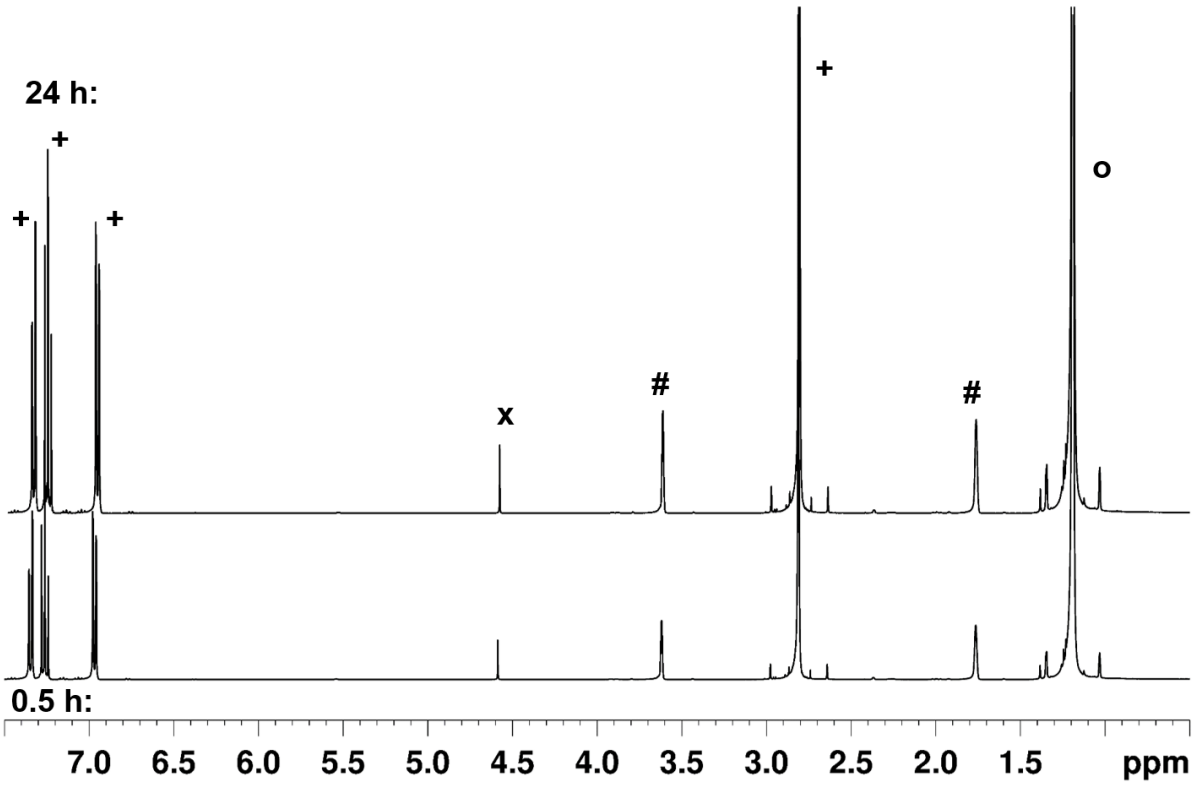

Figure S8. ^1H NMR spectra (400 MHz, d_8-THF (#), 26°C): Reaction mixture from $Ni(PMe_3)_4$ (**O**), N,N,N',N'-tetramethyl-1,8-diaminonaphthalene (base, +) under 1 atm of H_2 (**X**) after 0.5 h (*bottom*) and 24 h (*top*) at r.t.

Treatment of $[(Me_3P)_4Ni]NTf_2$ with H_2.

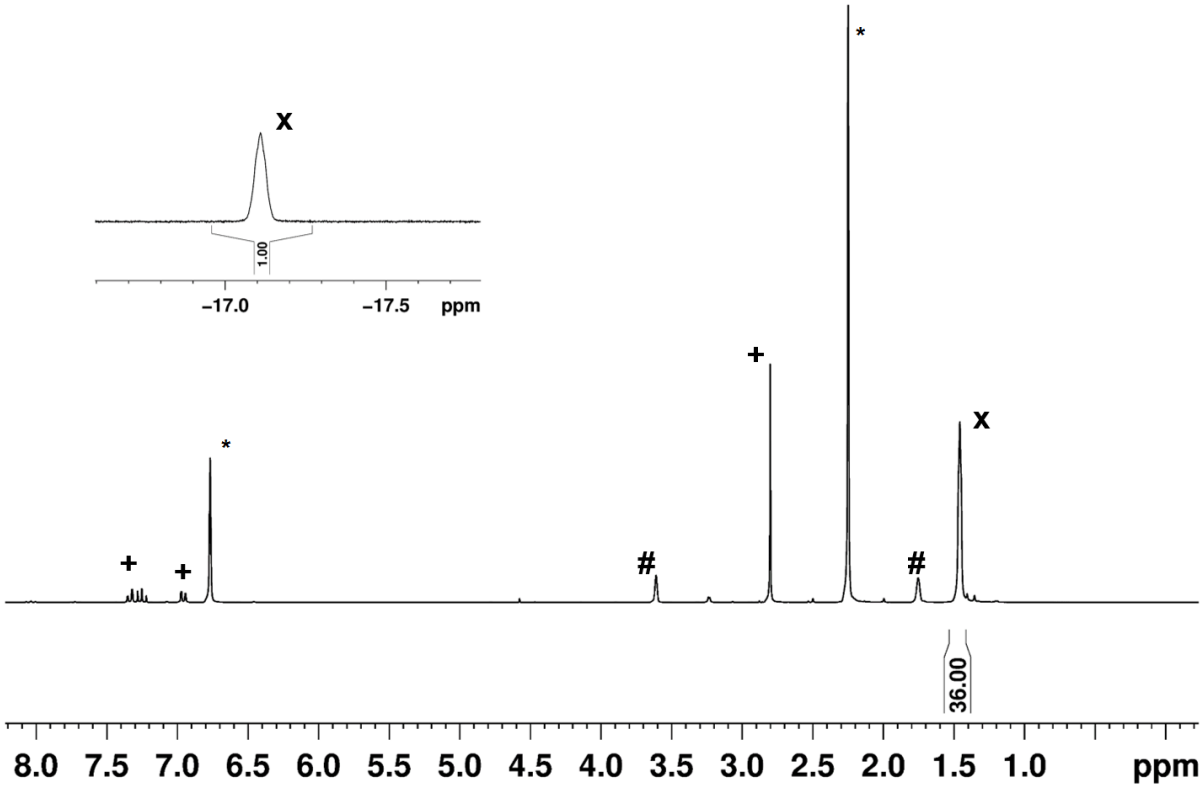

Figure S9. ^1H NMR spectrum (400 MHz, d_8-THF (#), 26°C): Reaction mixture from $[Ni(PMe_3)_4]^+$ (**X**) under 1 atm of H_2 in presence of N,N,N',N'-tetramethyl-1,8-diaminonaphthalene (base, +) after 7 days at r.t.; Mesitylene (*) used as internal standard; *Inset*: Ni-H resonance assigned to $[HNi(PMe_3)_4]^+$.

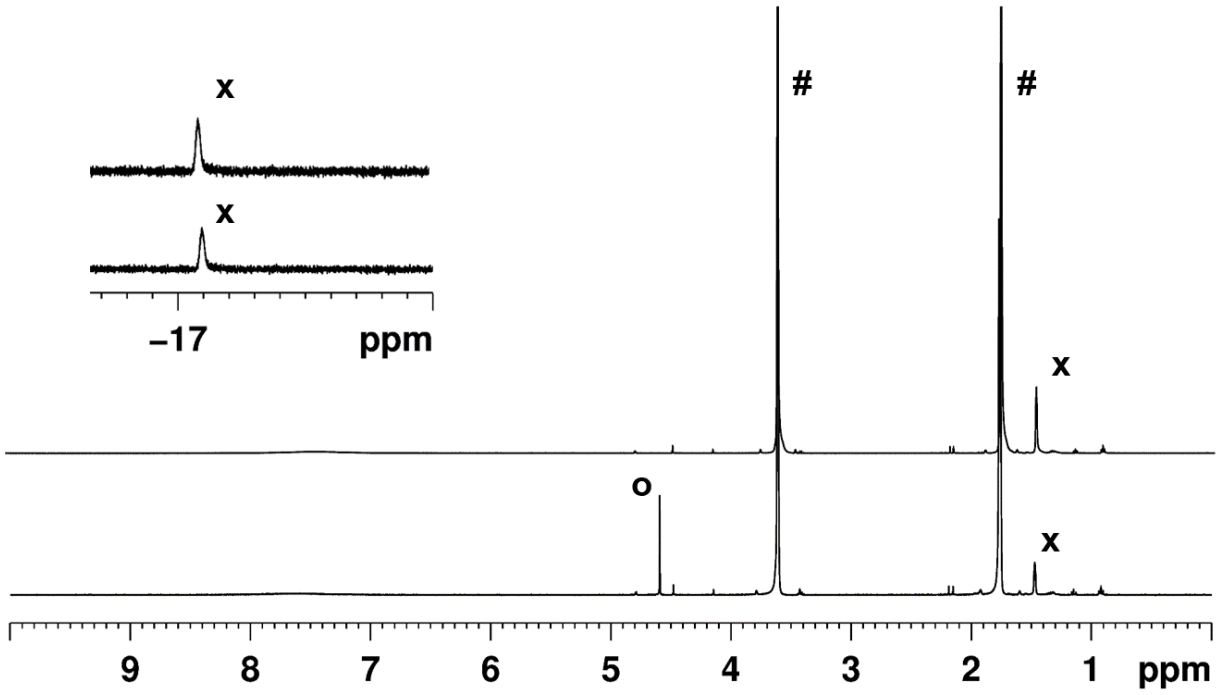

Figure S10. ^{1}H NMR spectra (400 MHz, d_8-THF (#), 26°C): Reaction mixture from $[Ni(PMe_3)_4]^+$ under 1 atm of H_2 (*bottom*), and after replacing H_2 by argon (*top*); Characteristic resonance of $[HNi(PMe_3)_4]^+$ (**X**). Inset: Characteristic resonance of $[^{\textit{H}}Ni(PMe_3)_4]^+$ (**X**) under 1 atm of H_2 (*bottom*), and after replacing H_2 by argon (*top*).

Treatment of $[(Me_3P)_4Ni]NTf_2$ with $Na[HB(OAc)_3]$.

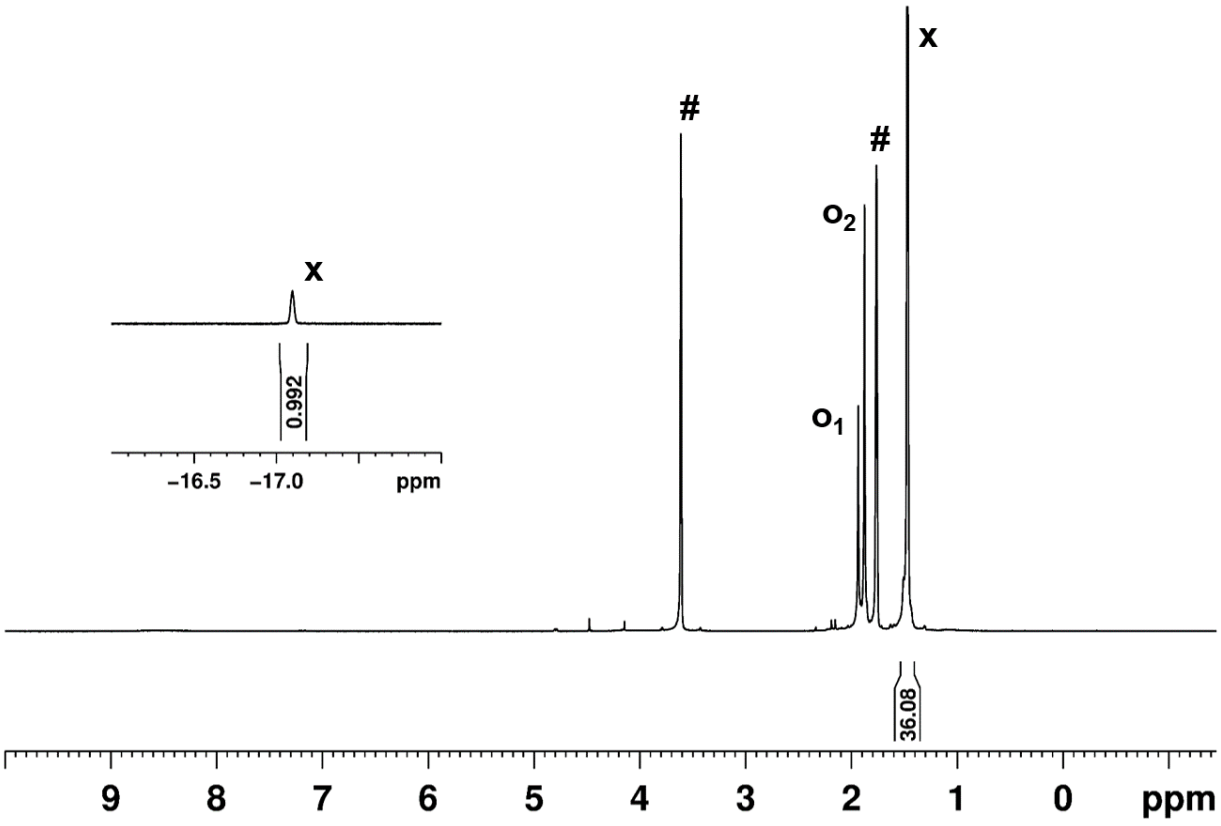

Figure S11. ^{1}H NMR spectrum (400 MHz, d_8-THF (#), 26°C): Reaction mixture from $[Ni(PMe)_4]^+$ and 0.5 equiv. of $Na[HB(OAc)_3]$; Characteristic resonances of $[HNi(PMe_3)_4]^+$ (**X**), unreacted $[HB(OAc)_3]^-$ (**O**$_1$), and $B(OAc)_3$ co-product (**O**$_2$).

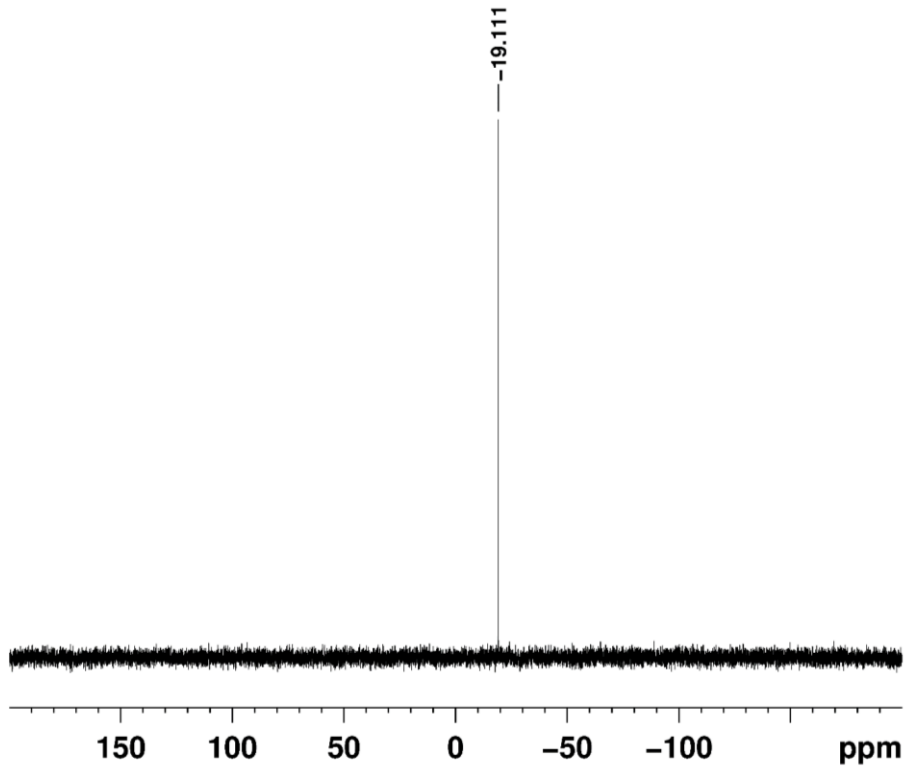

Figure S12. $^{31}P\{^{1}H\}$ NMR spectrum (162 MHz, d_8-THF (#), 26°C): Reaction mixture from $[Ni(PMe_3)_4]^+$ and 0.5 equiv. of $Na[HB(OAc)_3]$; δ_P = –19.1 ppm ($[HNi(PMe_3)_4]^+$).

H/D-Exchange in $[HNi(PMe_3)_4]NTf_2$.

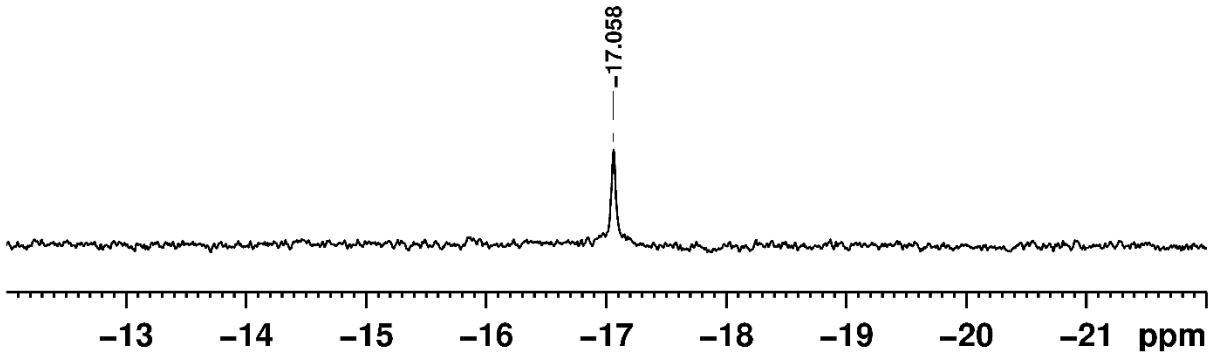

Figure S13. ^{2}H NMR spectrum (76 MHz, d_8-THF, 26°C): δ_D = –17.05 ppm ($[DNi(PMe_3)_4]^+$) owing to H-D exchange from $[HNi(PMe_3)_4]^+$ under 1 atm of D_2 at 24°C.

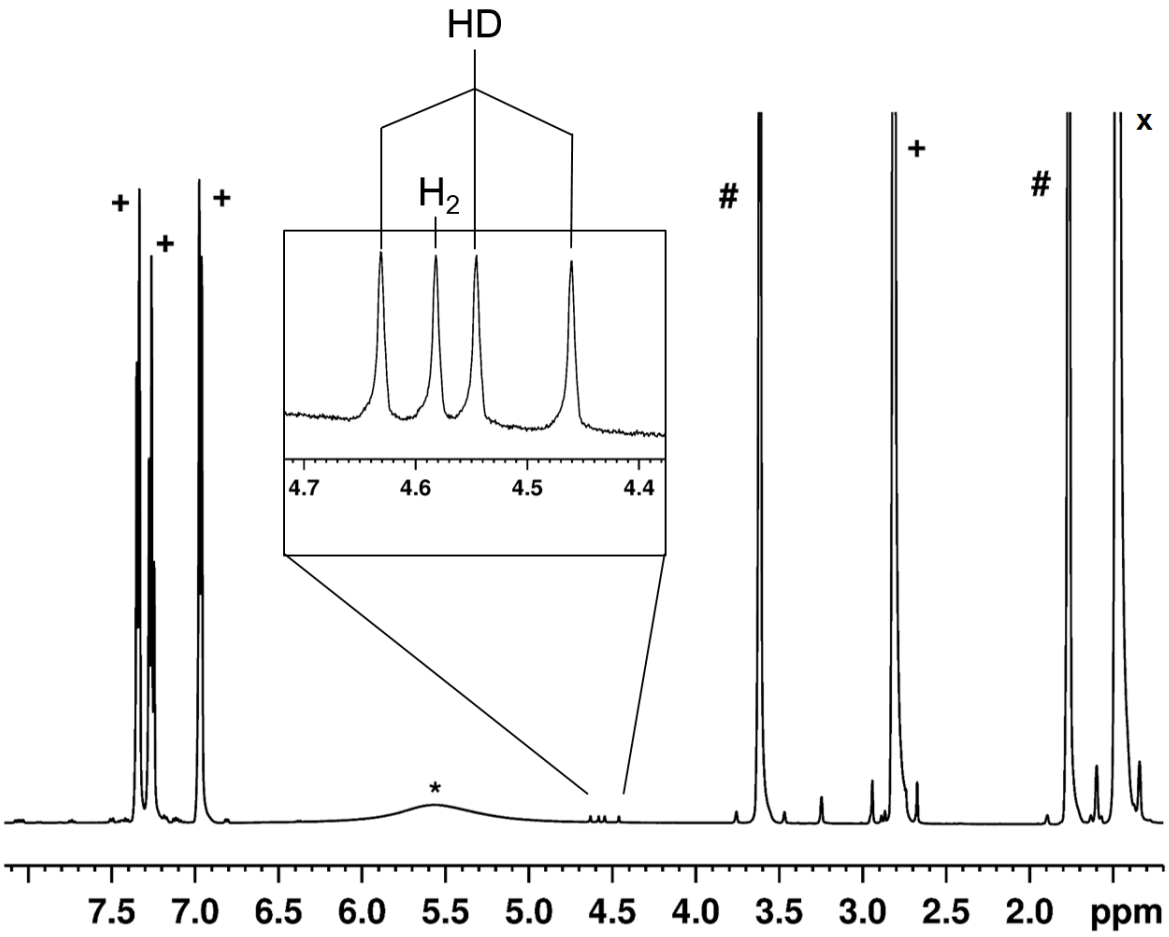

Figure S14. ^{1}H NMR spectrum (500 MHz, d_8-THF (#), 26°C): Reaction mixture from $[HNi(PMe_3)_4]^+$ (**X**) and 1 equiv. of N,N,N',N'-tetramethyl-1,8-diaminonaphthalene (base, +) under 1 atm of D_2; * denotes unknown species; *Inset*: δ_H = 4.58 (s, H_2), and 4.54 ppm (t, ^{1}J = 42.7 Hz, H-D).

Treatment of [2][NTf$_2$]$_2$ with 2 equiv. of [Hbase]$^+$. A solution of [**2**](NTf$_2$)$_2$ (20 mg, 0.014 mmol) and base (6 mg, 0.028 mmol) in CD_2Cl_2 (0.5 mL) was placed in a NMR tube. The reaction mixture was analysed by ^{1}H and ^{31}P{^{1}H} NMR spectroscopy at 26°C over a period of 24 h.

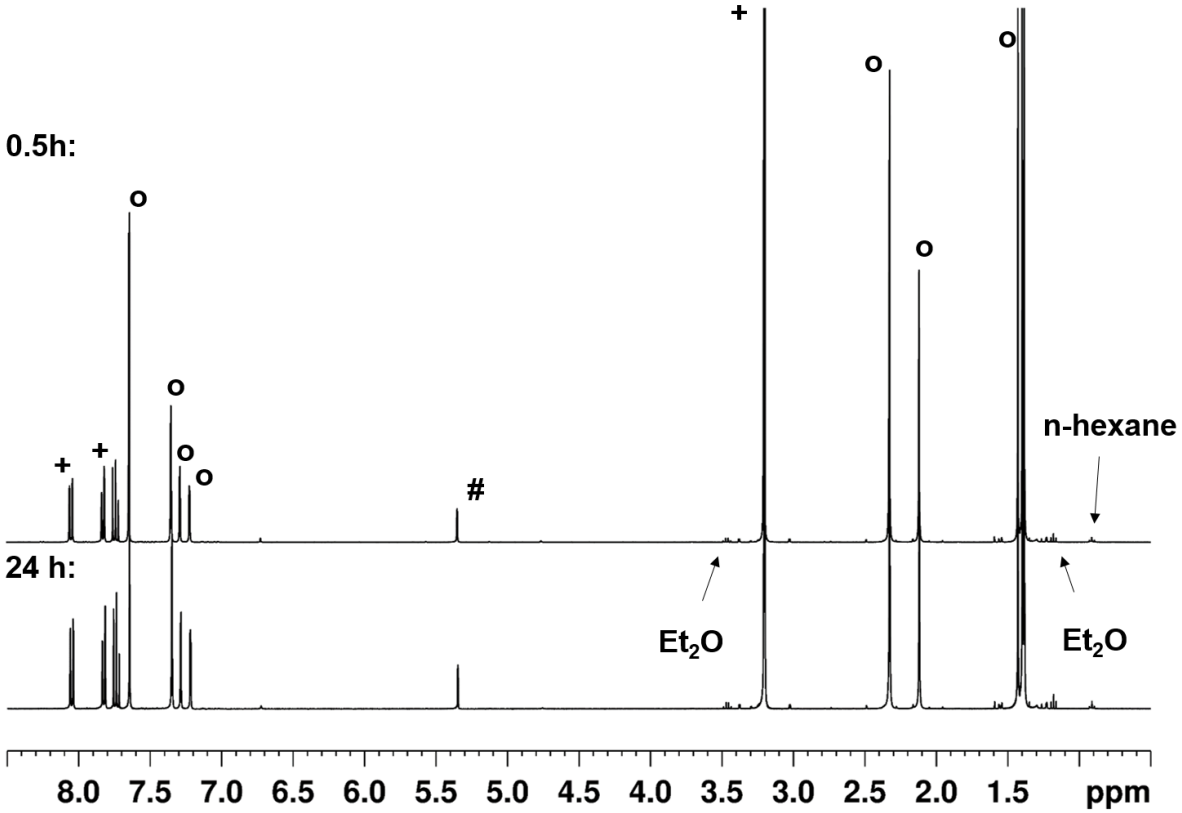

Figure S 15. ^{1}H NMR spectra (400 MHz, CD_2Cl_2 (#), 26°C): Reaction mixture of [**2**]$^{2+}$ (**O**) and 2 equiv. of [Hbase]$^+$ (+, base = N,N,N',N'-tetramethyl-1,8-diaminonaphthalene) after 30 minutes (*top*) and 24h (*bottom*); residual Et_2O and n-hexane from synthesis of [**2**](NTf$_2$)$_2$.

Treatment of [2][NTf$_2$]$_2$ with H$_2$. A solution of [**2**](NTf$_2$)$_2$ (20 mg, 0.014 mmol) and N,N,N',N'-tetramethyl-1,8-diaminonaphthalene (3 mg, 0.014 mmol) in CD_2Cl_2 (0.5 mL) was placed in a NMR tube. The solution was degassed three times by freeze-pump-thaw technique and the evacuated tube was set under 4 atm of H_2. Reaction progress was monitored by ^1H and $^{31}P\{^1H\}$ NMR spectroscopy at 26°C.

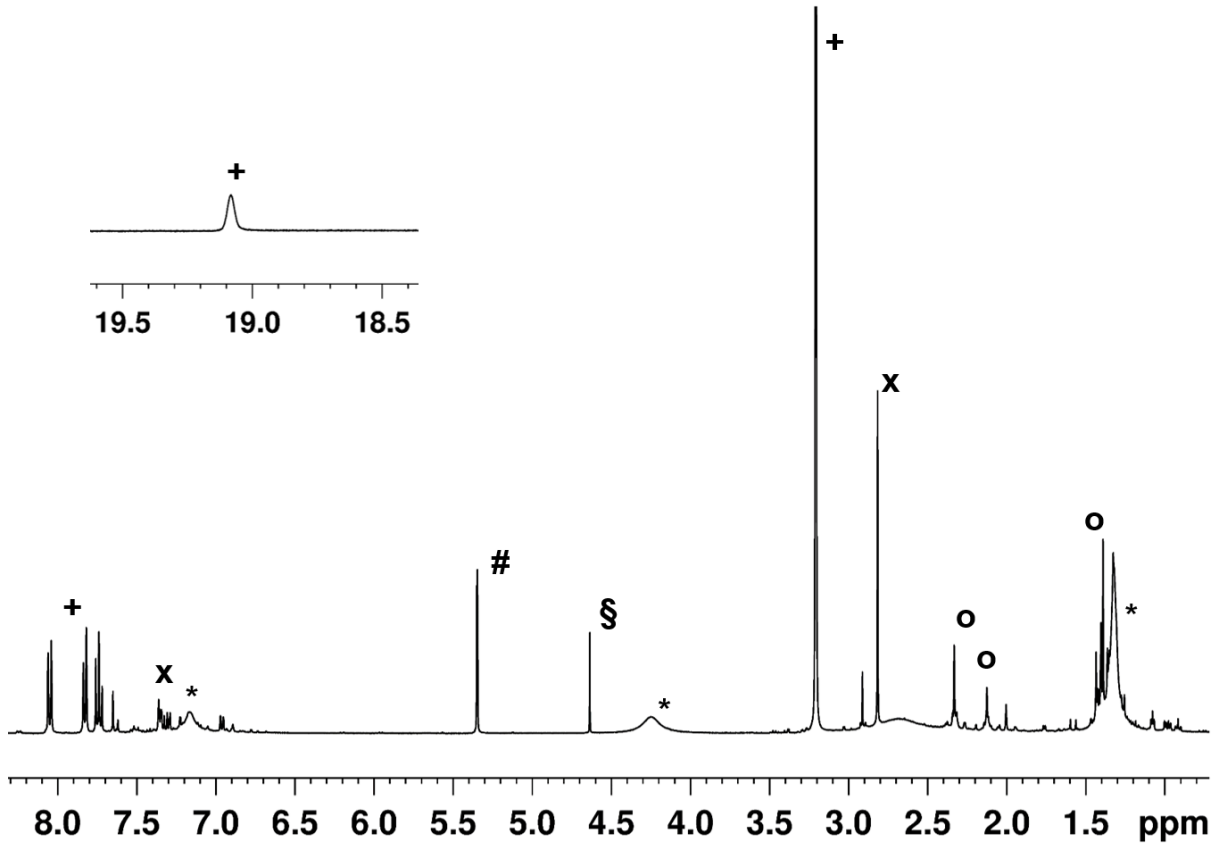

Figure S16. ^1H NMR spectrum (400 MHz, CD_2Cl_2 (#), 26°C): Reaction mixture from [**2**]$^{2+}$, 1 equiv. of N,N,N',N'-tetramethyl-1,8-diaminonaphthalene (base, **X**) under 4 atm of H_2 after 70 minutes of reaction time; ***** = [**1**]$^+$, **O** = [**2**]$^{2+}$, **§** = H_2, **+** = [Hbase]$^+$; *Inset*: δ_H = 19.1 ppm (s, [*H*base]$^+$).

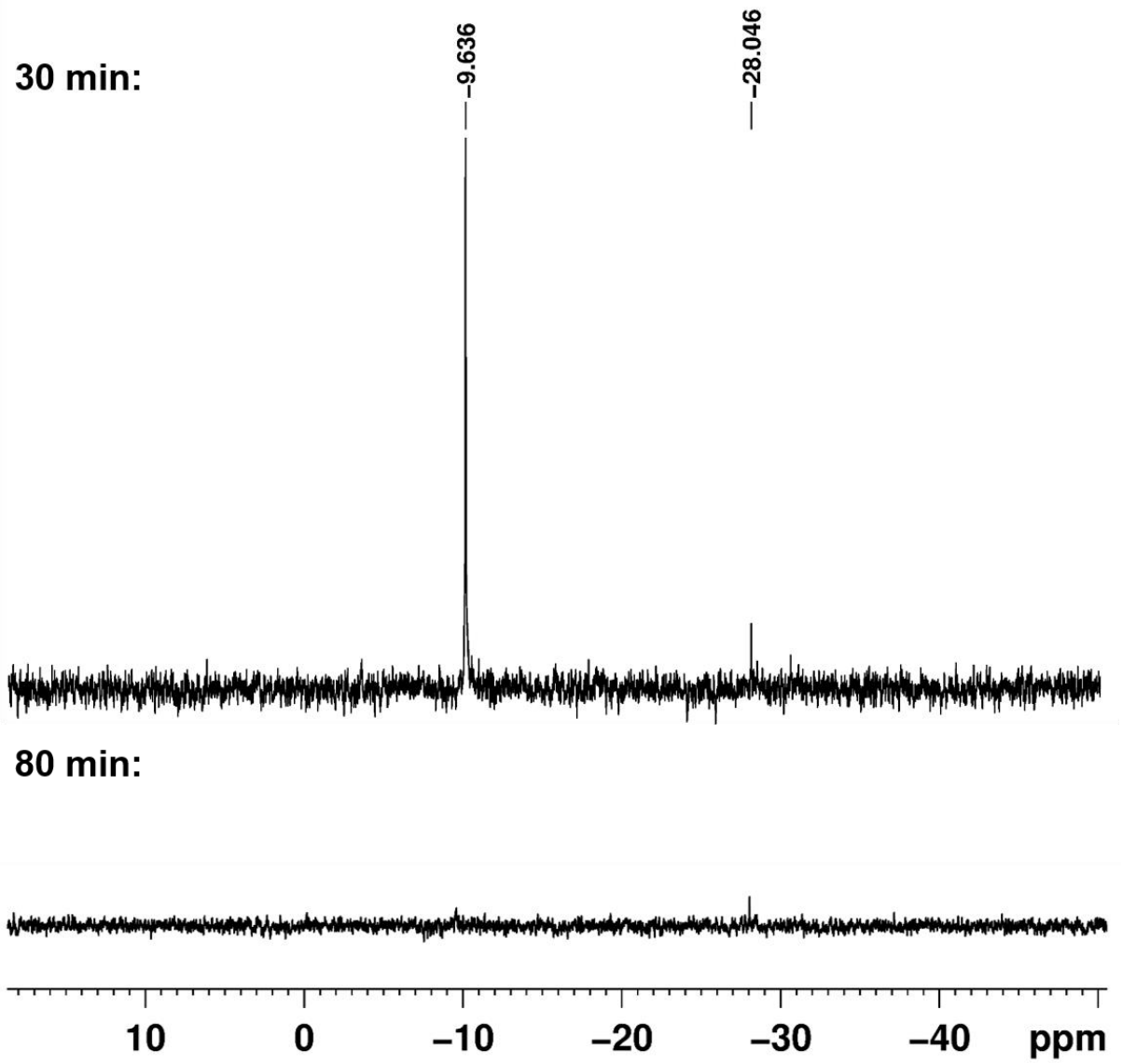

Figure S17. $^{31}P\{^{1}H\}$ NMR spectra (162 MHz, CD_2Cl_2, 26°C): Reaction mixture from $[\mathbf{2}]^{2+}$ and 1 equiv. of N,N,N',N'-tetramethyl-1,8-diaminonaphthalene under 4 atm of H_2 after 30 (*top*) and 80 min (*bottom*) at r.t.; δ_P = –9.6 ($[\mathbf{2}]^{2+}$), and –28 ppm (co-product **3**).

Treatment of [2](NTf$_2$)$_2$ with H$_2$ in the presence of a stoichiometric amount of [HNi(PMe$_3$)$_4$]NTf$_2$.

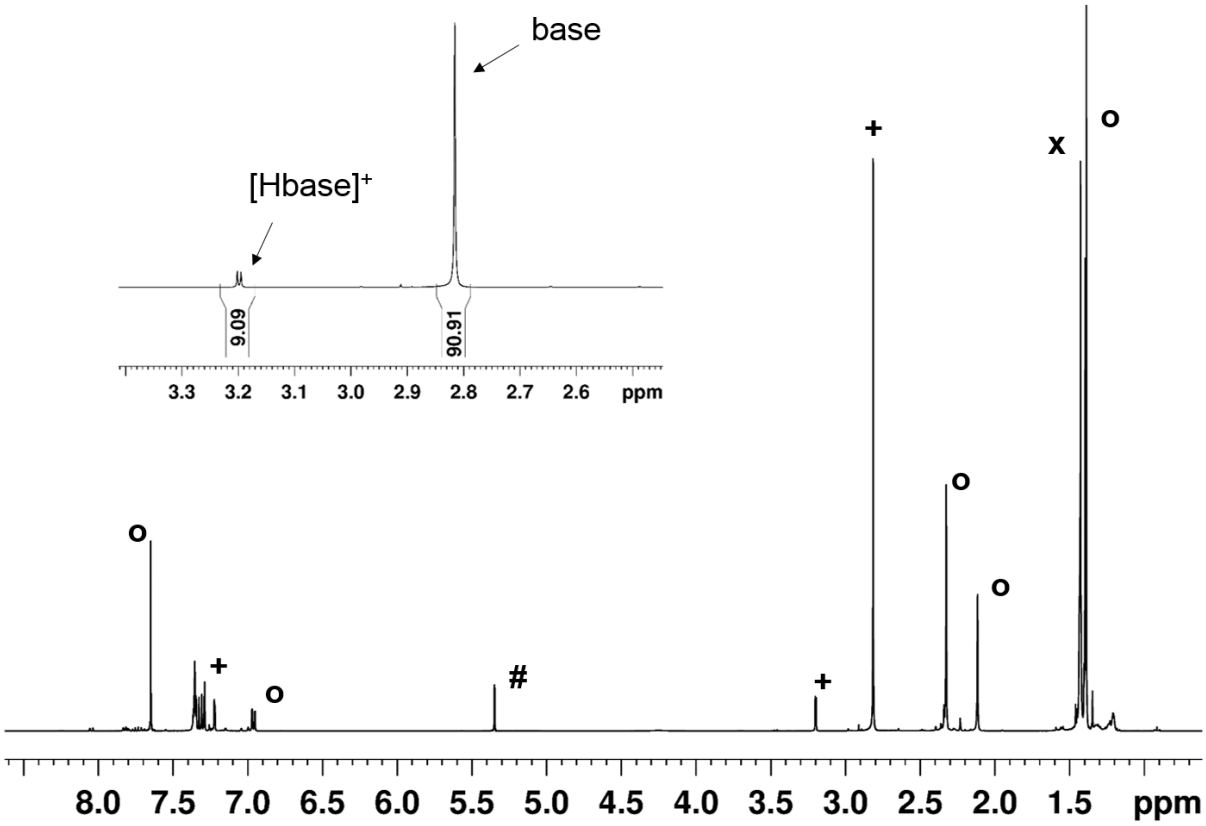

Figure S18. ^{1}H NMR spectrum (400 MHz, CD_2Cl_2, (#), 26°C): Reaction mixture from [**2**]$^{2+}$, 1 equiv. of N,N,N',N'-tetramethyl-1,8-diaminonaphthalene (base, +), and 0.5 equiv. of [HNi(PMe$_3$)$_4$]$^+$ after 30 min. at r.t.; **O** = [**2**]$^{2+}$, **X** = [HNi(PMe$_3$)$_4$]$^+$; *Inset*: δ_H = 2.81 (base), and 3.19 (d, ^3J = 2.7 Hz, [Hbase]$^+$), corresponding to a 10 % conversion.

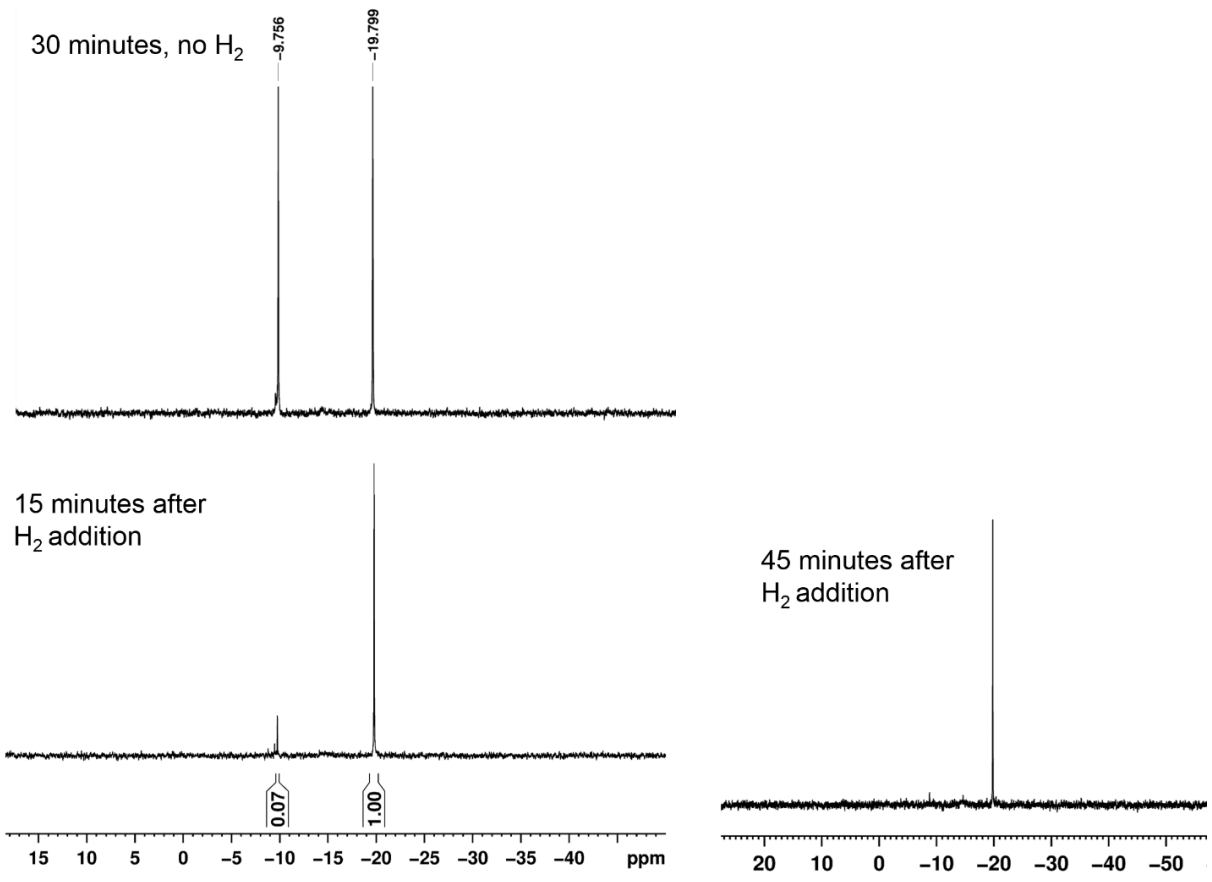

Figure S19. $^{31}P\{^{1}H\}$ NMR spectra (162 MHz, CD_2Cl_2, 26°C): Reaction mixture composed of $[\mathbf{2}]^{2+}$, 1 equiv. of N,N,N',N'-tetramethyl-1,8-diaminonaphthalene, and 0.5 equiv. of $[HNi(PMe_3)_4]^+$ after 30 min under argon (*top left*), 15 min under 1 atm of H_2 (*bottom left*), and 45 min under 1 atm of H_2 (*bottom right*) at r.t.; δ_P = –9.7 ($[\mathbf{2}]^{2+}$), and –19.8 ppm ($[HNi(PMe_3)_4]^+$).

Stoichiometric Reaction of [1]NTf_2 and [$HNi(PMe_3)_4$]NTf_2 under H_2/argon.

A solution of [**1**]NTf_2 (28.0 mg, 0.023 mmol), N,N,N',N'-tetramethyl-1,8-diaminonaphthalene (base, 5 mg, 0.023 mmol), and [$HNi(PMe_3)_4$]NTf_2 (15 mg, 0.023 mmol) in 1 mL CD_2Cl_2 was split into two NMR samples. One of the samples was degassed by three freeze-pump-thaw cycles and exposed to 1 atm of H_2 whereas the other sample was kept under argon. Reaction progress was monitored by ^{1}H NMR spectroscopy.

Table S1. Conversion of N,N,N',N'-tetramethyl-1,8-diaminonaphthalene with reaction time under an atmosphere of H_2/argon.

reaction time	%-conversion under argon	%-conversion under H_2
0.5 h	7 ± 5	20 ± 5
2 h	16 ± 5	40 ± 5
5 h	48 ± 5	65 ± 5
21 h	80 ± 5	95 ± 5

3. UV/vis Data

General information on stoichiometric H_2 oxidation by [2](NTf$_2$)$_2$. The conversion of [**2**](NTf$_2$)$_2$ into [**1**]NTf$_2$ under 1 atm of H_2 with time was quantified by UV/vis spectroscopy from samples prepared *in situ* in a gas tight, four-side transparent, fused quartz cuvette connected to a 10 mL round bottom flask (Figure S20). Reactant solutions were prepared and transferred to the apparatus inside a glove box, degassed by three freeze-pump-thaw cycles and exposed to 1 atm of H_2 using the round bottom compartment, and finally decanted into the cuvette after warming to r.t. Temperature was kept constant at T = 297 K using a thermostat, and magnetic stirring was stopped during data acquisition.

Figure S20. Apparatus of four-sided quartz cuvette connected to a 10 mL round bottom flask for quantitative monitoring of H_2 oxidation by UV/vis spectroscopy.

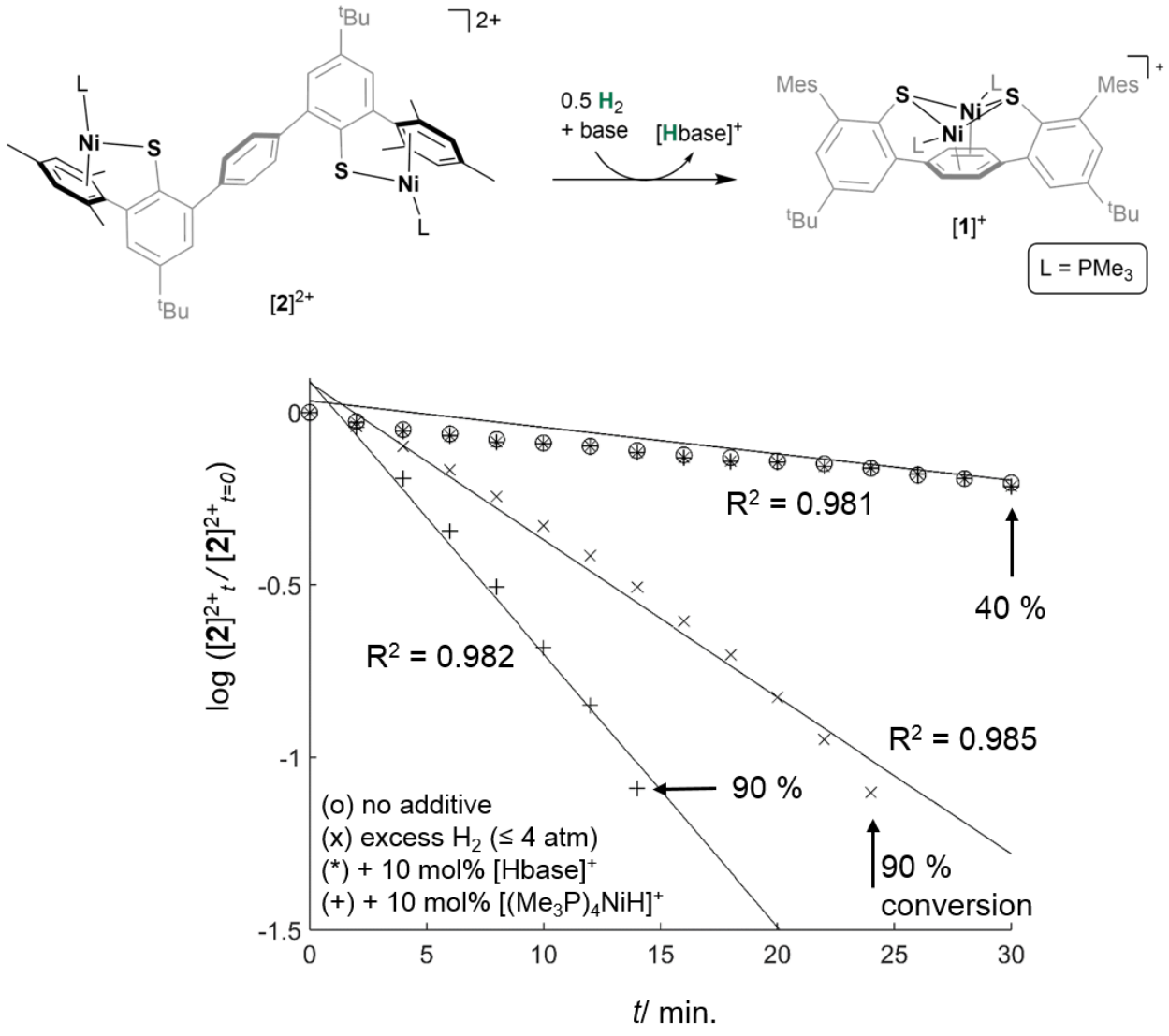

Figure S21. Logarithmic plots of normalized concentrations of $[\mathbf{2}]^{2+}$ vs time under the following conditions: (**o**) $P(H_2) \leq 1$ atm; (**x**) $P(H_2) \leq 4$ atm; (*) $P(H_2) \leq 1$ atm/1 equiv. of $[Hbase]^+$; (+) $P(H_2) \leq 1$ atm/10 mol-% $[HNi(PMe_3)_4]^+$; k_{obs} calculated from linear regressions: (o) = (*) = 1.3, (x) = 7.2, (+) = 12.3×10^{-4}. Details of each run are provided in Figures S22-S30.

Reaction under $P(H_2) \leq 4$ atm. 4 mL of a 0.143 mM stock solution of [**2**]$(NTf_2)_2$ in CH_2Cl_2 and 0.033 mL of a 16.98 mM stock solution of N,N,N',N'-tetrametyl-1,8-naphthalenediamine (proton sponge = base) in C_6H_6 were combined and degassed as described. H_2 was admitted to the sample at −196°C. Reaction started after careful warming to r.t., and spectra were collected every two minutes for 2 hours. The experiment was repeated twice, and an averaged first order plot is shown in Figure S21.

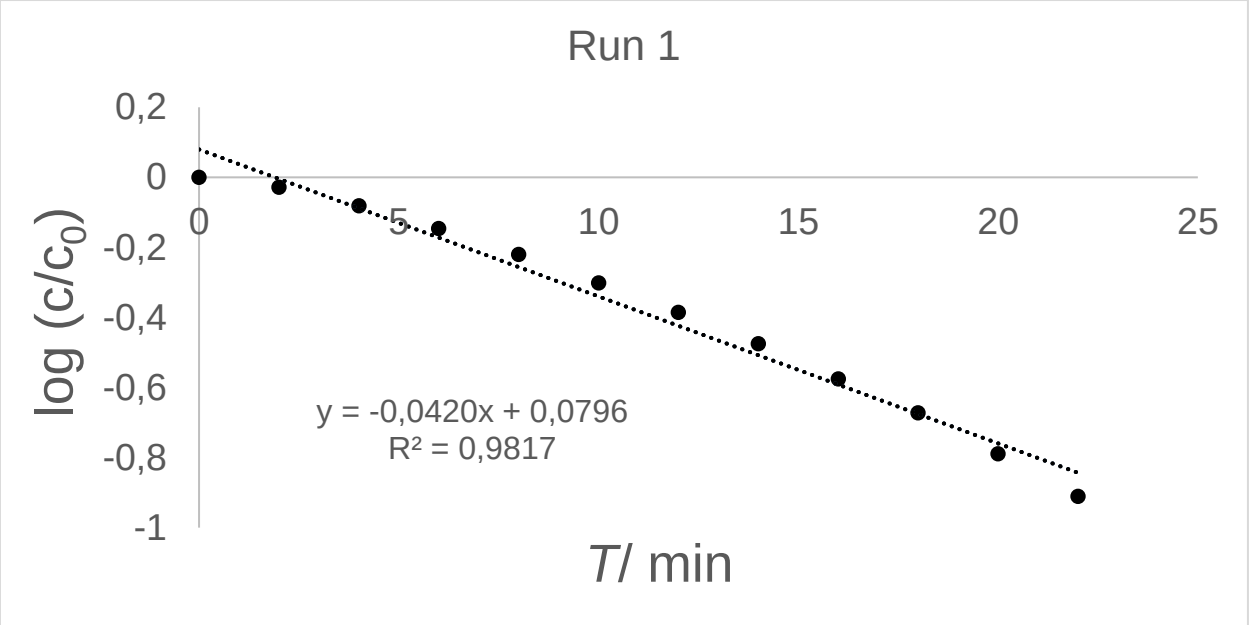

Figure S22. Plot of $\log([\mathbf{2}]^{2+}_t/[\mathbf{2}]^{2+}_{t=0})$ vs time under $P(H_2) \leq 4$ atm, $k_{obs}(24°C)$ = –slope/60 = 7×10^{-4} s^{-1}.

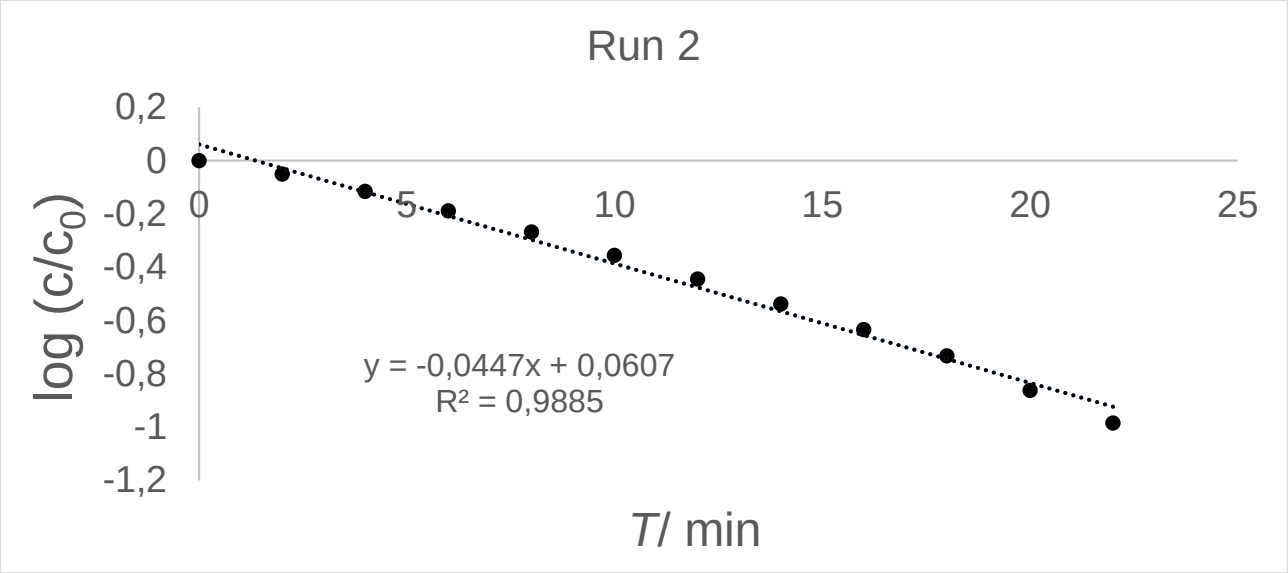

Figure S23. Plot of $\log([\mathbf{2}]^{2+}_{t}/[\mathbf{2}]^{2+}_{t=0})$ vs time under $P(H_2) \leq 4$ atm, $k_{obs}(24°C) = -\text{slope}/60 = 8 \times 10^{-4}\ s^{-1}$.

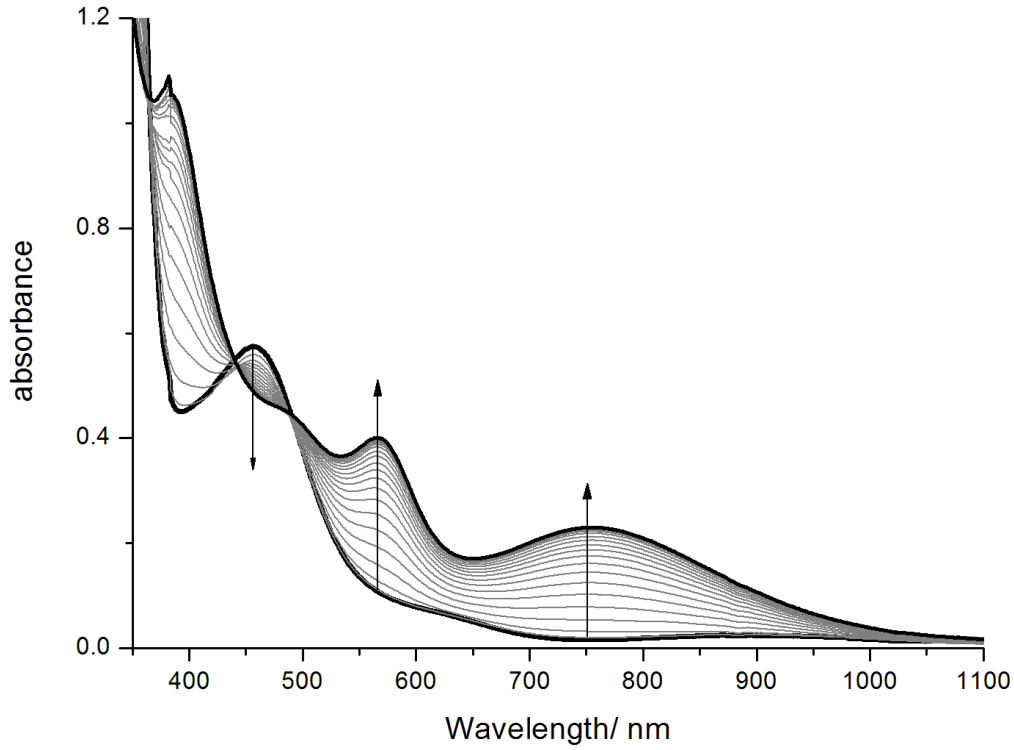

Figure S24. Representative example of time dependent conversion of [**2**](NTf$_2$)$_2$ into [**1**]NTf$_2$ in the presence of 1 equiv. of base under $P(H_2) \leq 4$ atm in CH_2Cl_2 solution at $T = 24°C$ as monitored by UV/vis spectroscopy at time intervals = 2 min.

Reaction under $P(H_2)$ = 1 atm. 4 mL of a 0.136 mM stock solution of [**2**][NTf_2]$_2$ in CH_2Cl_2 and 0.032 mL of a 16.98 mM stock solution of base in C_6H_6 were combined, degassed, warmed to r.t. and exposed to 1 atm of H_2. Decrease of electronic transition at $\lambda(\varepsilon/M^{-1}\ cm^{-1})$ = 460 (5000) nm was probed every two minutes.

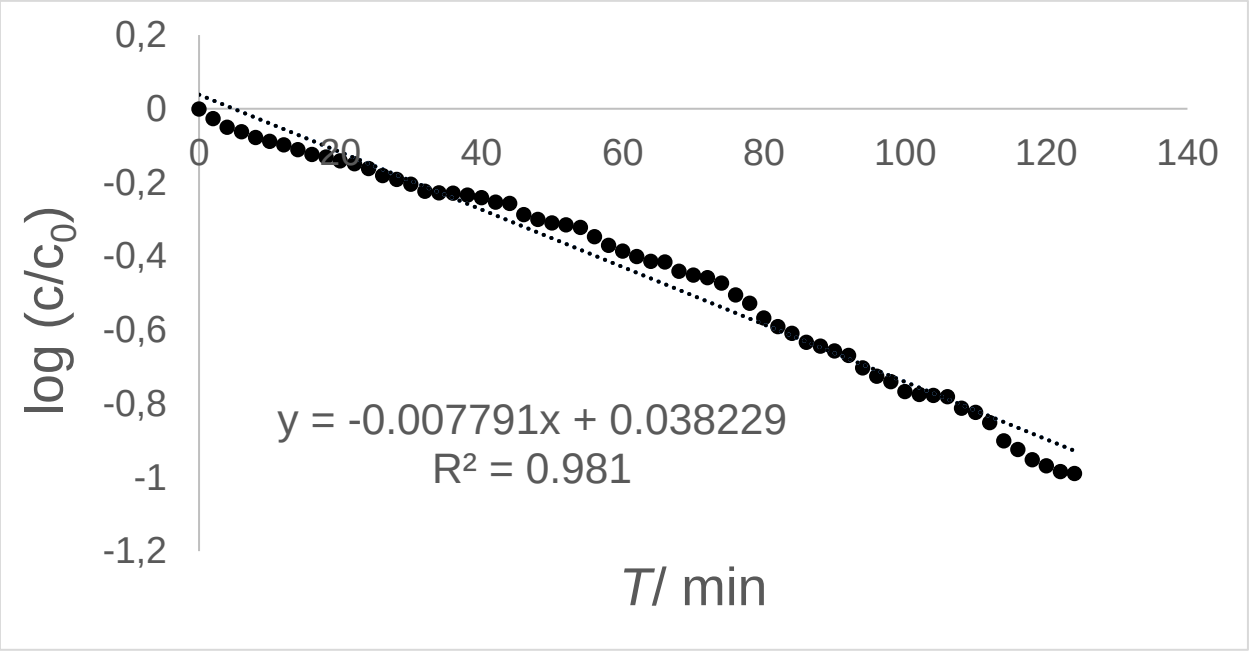

Figure S25. Plot of $\log([\mathbf{2}]^{2+}_t/[\mathbf{2}]^{2+}_{t=0})$ vs time under $P(H_2)$ = 1 atm, k_{obs}(24°C) = –slope/60 = $1.3 \times 10^{-4}\ s^{-1}$.

Effect of [HNi(PMe$_3$)$_4$]NTf$_2$ as additive. 4 mL of a 0.136 mM stock solution of [**2**](NTf$_2$)$_2$ in CH_2Cl_2, 32 μL of a 16.98 mM stock solution of base in C_6D_6, and 6 μL of a 9.34 mM stock solution of [HNi(PMe$_3$)$_4$]NTf$_2$ in C_6H_6 were combined, degassed, warmed to r.t., and finally exposed to 1 atm of H_2. UV/vis spectra were collected every two minutes over a period of 1 h. This experiment was repeated two times and an averaged logarithmic plot is shown Figure 2 in the main text.

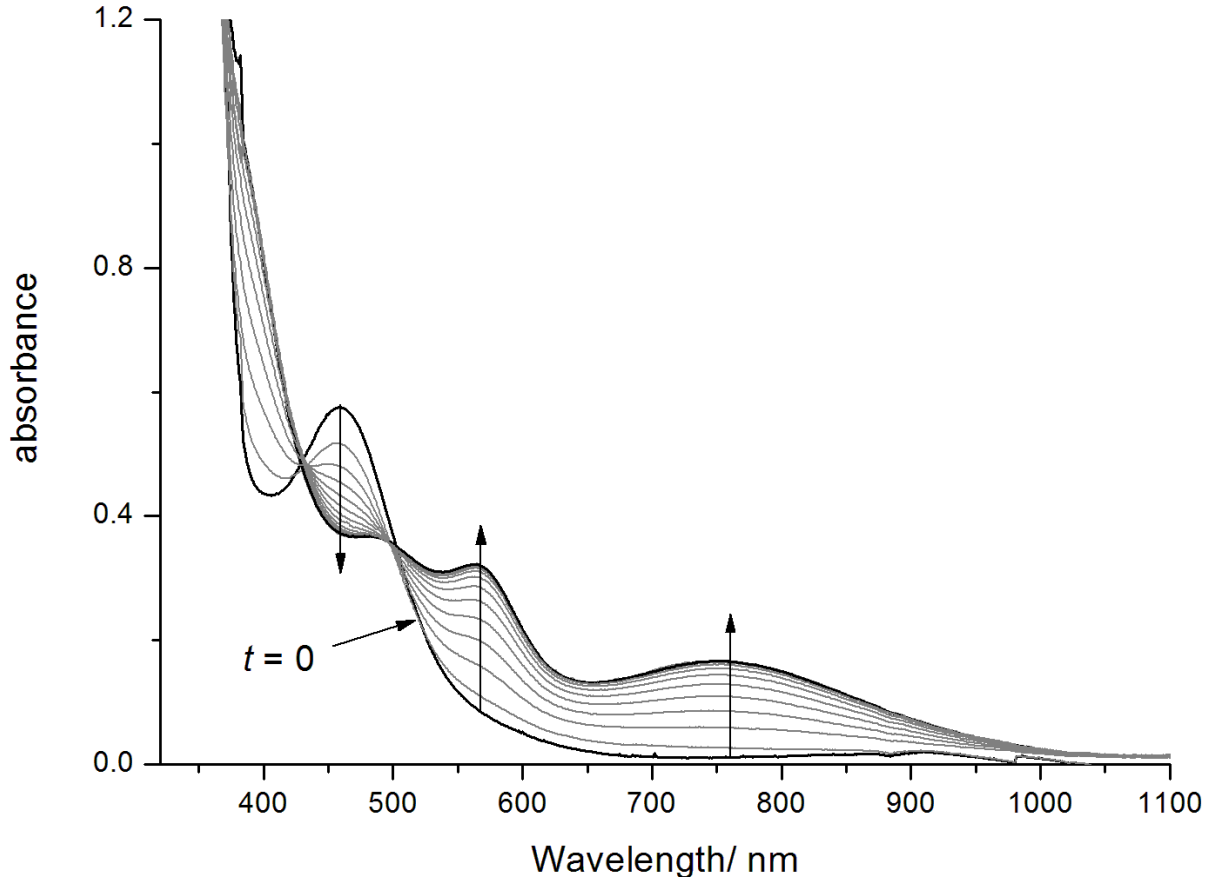

Figure S26. Representative example of time dependent conversion of [**2**](NTf$_2$)$_2$ into [**1**]NTf$_2$ in the presence of 1 equiv. of base, and 10 mol-% of [HNi(PMe$_3$)$_4$]NTf$_2$ under $P(H_2) \leq 4$ atm in CH_2Cl_2 solution at $T = 24$°C as monitored by UV/vis spectroscopy at time intervals = 2 min.

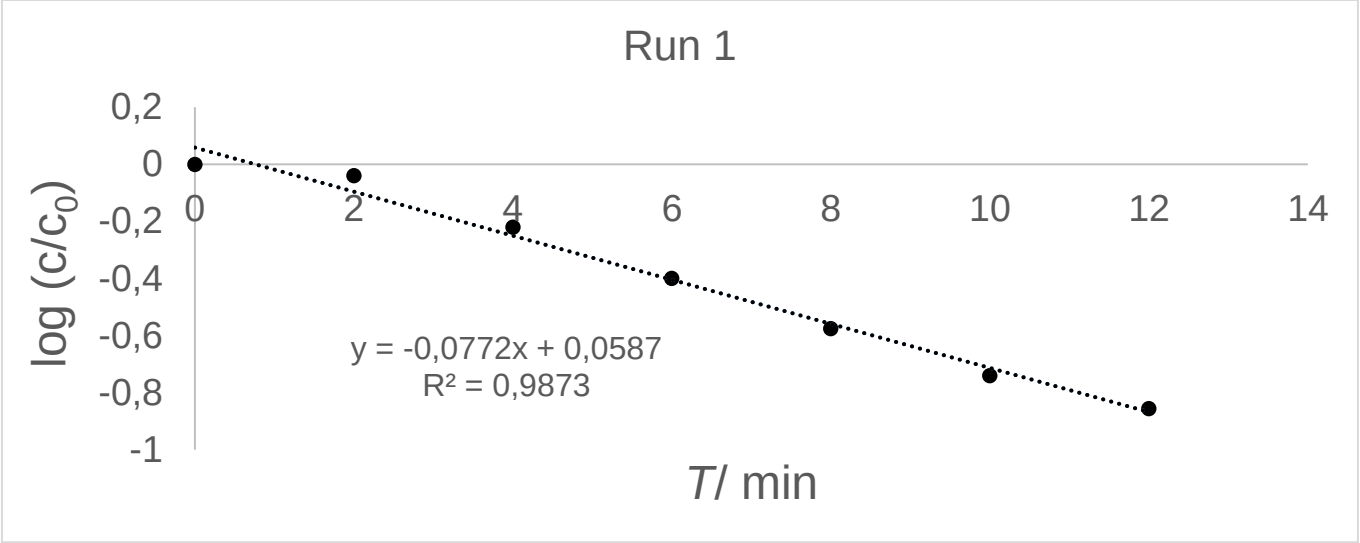

Figure S27. Plot of $\log([\mathbf{2}]^{2+}_{t}/[\mathbf{2}]^{2+}_{t=0})$ vs time under $P(H_2)$ = 1 atm in the presence of 10 mol-% of $[HNi(PMe_3)_4]NTf_2$ in CH_2Cl_2 solution; $k_{obs}(24°C)$ = –slope/60 = 1.3×10^{-3} s^{-1}.

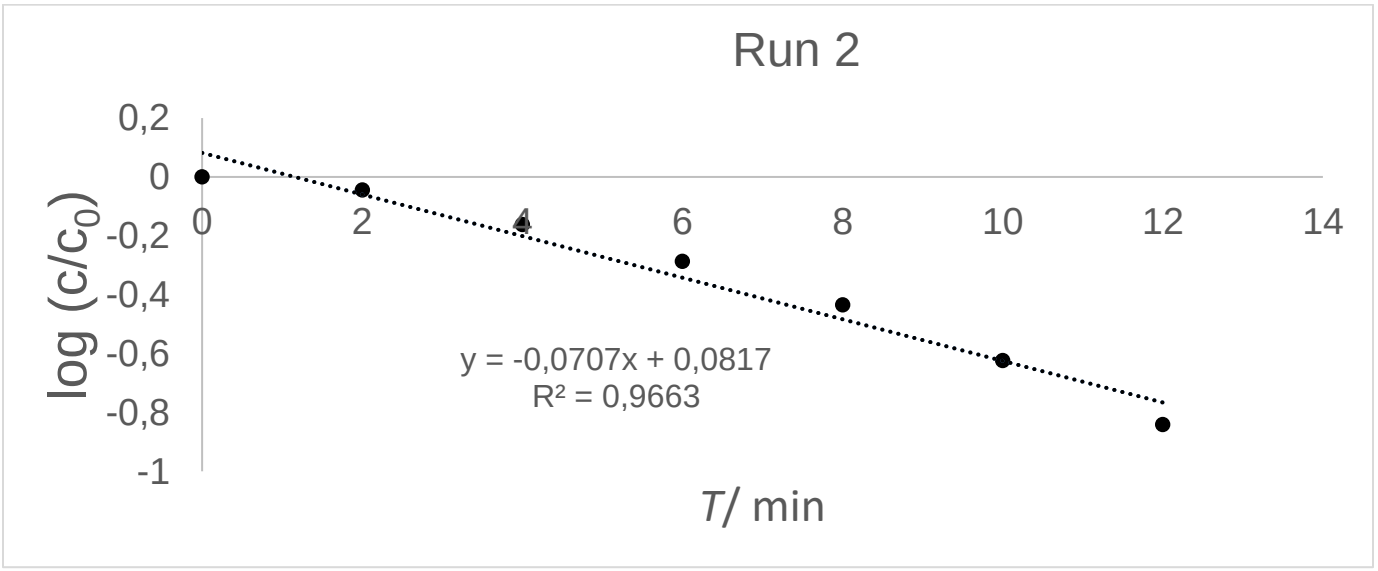

Figure S28. Plot of $\log([\mathbf{2}]^{2+}_{t}/[\mathbf{2}]^{2+}_{t=0})$ vs time under $P(H_2)$ = 1 atm in the presence of 10 mol-% of $[HNi(PMe_3)_4]NTf_2$ in CH_2Cl_2 solution; $k_{obs}(24°C)$ = –slope/60 = 1.2×10^{-3} s^{-1}.

Effect of [Ni(PMe$_3$)$_4$]NTf$_2$ as additive. 4 mL of a 0.136 mM stock solution of [**2**][NTf$_2$]$_2$ in CH_2Cl_2, 27 µL of a 17.15 mM stock solution of base in C_6H_6, and 6 µL of a 8.33 mM stock solution of [Ni(PMe$_3$)$_4$]NTf$_2$ in 1,2-$C_6H_4F_2$ were combined, degassed, and exposed to $P(H_2)$ = 1 atm. UV/vis spectra were collected every two minutes over a period of 2 hours.

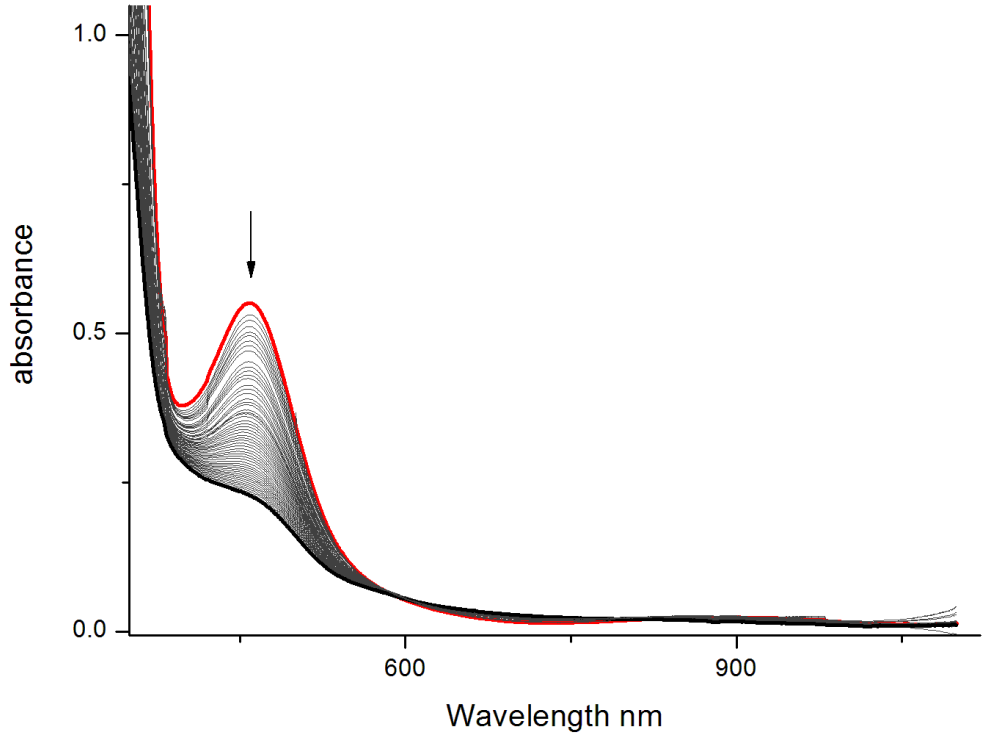

Figure S29. Series of UV/vis spectra taken at Δt = 2 min (solid red: t = 0) that show the consumption of [**2**]$^{2+}$ in the presence of 1 equiv. of base and 10 mol-% of [Ni(PMe$_3$)$_4$]NTf$_2$ under $P(H_2)$ = 1 atm. Only decomposition of the starting material is evident.

Effect of [HBase]$^+$ as additive. 4 mL of a 0.136 mM stock solution of [**2**][NTf_2]$_2$ in CH_2Cl_2, 32 μL of a 16.98 mM stock solution of base in C_6H_6, and 4 μL of a 0.0129 M stock solution of [HBase]NTf_2 in C_6H_6 were combined, degassed, warmed to r.t., and exposed to 1 atm of H_2. Decrease of electronic transition at $\lambda(\varepsilon/M^{-1}\ cm^{-1}) = 460\ (5000)$ nm was probed every two minutes.

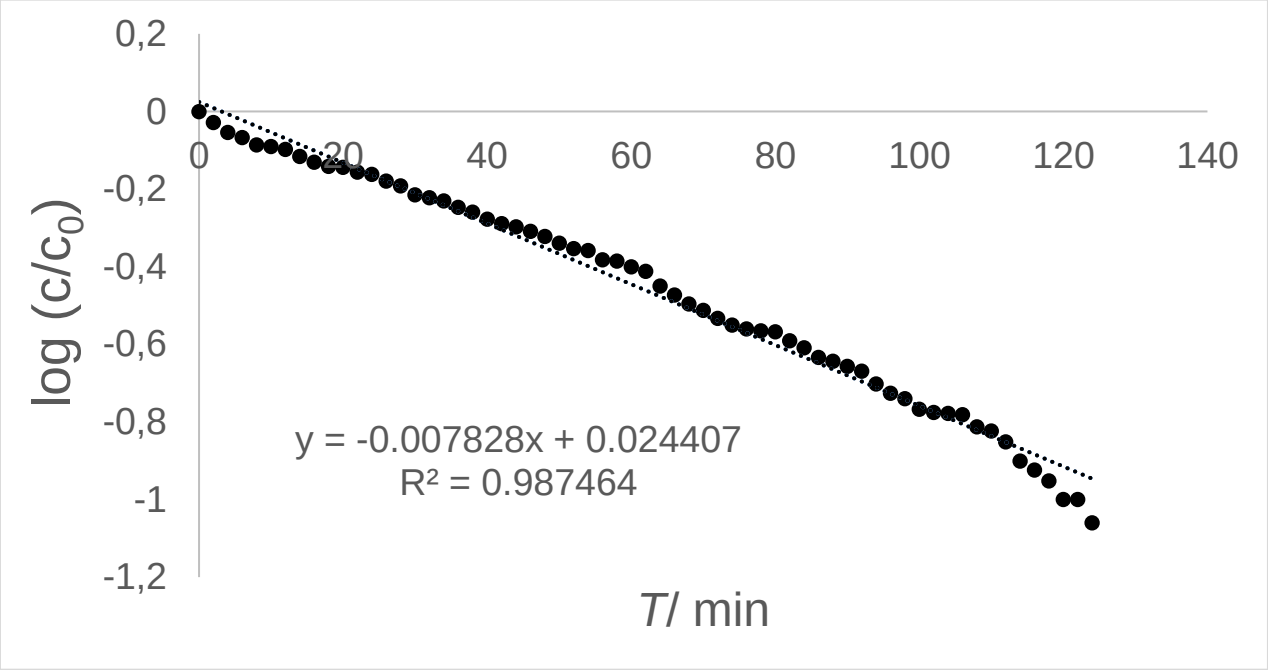

Figure S30. Plot of log([**2**]$^{2+}_t$/[**2**]$^{2+}_{t=0}$) vs time under $P(H_2)$ = 1 atm of H_2 in the presence of 10 mol-% of [Hbase]$^+$; k_{obs}(24°C) = –slope/60 = 1.3×10^{-4} s^{-1}.

4. Additional Kinetic Data for H_2 Oxidation by [2](NTf$_2$)$_2$.

The overall rate of H_2 oxidation is best described by a first order dependence in $[[\mathbf{2}]^{2+}]_t$

$$\nu \approx k_{obs1} \times [[\mathbf{2}]^{2+}]_t$$

Under the condition that deliberately added $[HNi(PMe_3)_4]^+$ acts as catalyst, $[[HNi(PMe_3)_4]^+]_t \approx [[HNi(PMe_3)_4]^+]_0$ which gives

$$\nu \approx k_{obs2} \times [[HNi(PMe_3)_4]^+]_0 \times [[\mathbf{2}]^{2+}]_t$$

For $[[\mathbf{2}]^{2+}]_0 = 0.136$, and $[[HNi(PMe_3)_4]^+]_0 = 0.014$ mmol/L, $k_{obs2} = 1.2 \times 10^{-3}$ s^{-1} (average from linear regressions in Figures S27-S28). Correction for $[[HNi(PMe_3)_4]^+]_0 = 0.014$ mmol/L yields $k_{cat} = 8.6 \times 10^{-3}$ s^{-1}·L·mol^{-1}.

For reactions with no added $[HNi(PMe_3)_4]^+$, $k_{obs1} = 1.3 \times 10^{-4}$ s^{-1} (from linear regression in Figure S25). A concentration of *potentially* formed $[HNi(PMe_3)_4]^+$ is estimated as follows:

$$[[HNi(PMe_3)_4]^+] = k_{obs1}/k_{cat} = 0.0015 \text{ mmol/ L.}$$

Since formation of $[HNi(PMe_3)_4]^+$ consumes 2 equiv. of $[\mathbf{2}]^{2+}$ this corresponds to $2[[HNi(PMe_3)_4]^+]/[[\mathbf{2}^{2+}]]_0 \approx 0.003/0.136 = 0.022$ or $\leq$ **2 %**.

5. Determination of pK_a(1,2-$C_6H_4F_2$) of $[HNi(PMe_3)_4]^+$.

A solution of $[HNi(PMe_3)_4]NTf_2$ (14.9 mg, 0.023 mmol) and N,N,N',N'-tetramethyl-1,8-diaminonaphthalene (4.7 mg, 0.022 mmol) in 1,2-$C_6H_4F_2$ (0.5 mL) and C_6D_6 (90 mg) was prepared in an NMR tube. A ^1H NMR spectrum was recorded and the equilibrium molar ratio of $[Hbase]^+/([base]+[Hbase]^+)$ calculated from integrated peak areas. The value used for calculation is the average from spectra recorded after t = 0.25 and 23 h.

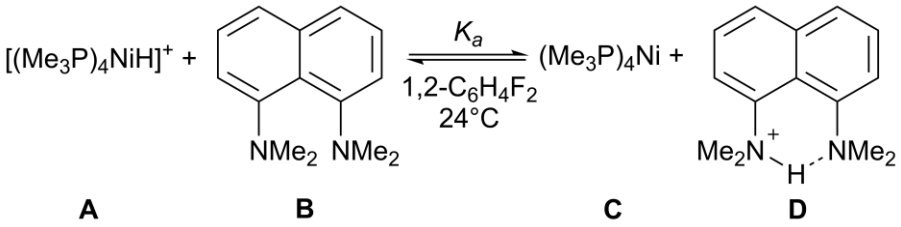

$$K_a(1,2\text{-}C_6H_4F_2) = \frac{[C][D]}{[A][B]}$$

$[D]/([B]+[D]) = [D]/[B]_0 = 0.0035$

$[D] = 0.0035 \times [B_0] = 0.00015$ mol/L

$[A] = [A_0] - [D] = (0.04627 - 0.00015)$ mol/L $= 0.04612$ mol/L

$[B] = [B_0] - [D] = (0.04392 - 0.00015)$ mol/L $= 0.04377$ mol/L

$[C] = [D] = 0.00015$ mol/L

$$K_a(1,2\text{-}C_6H_4F_2) = \frac{0.00015^2}{0.04612 \cdot 0.04377}\frac{mol^2L^2}{mol^2L^2} = 1.1 \cdot 10^{-5}$$

$$pK_a(1,2\text{-}C_6H_4F_2) = -logK_a = 5$$

6. Supplementary CV Data of $Ni(PMe_3)_4$.

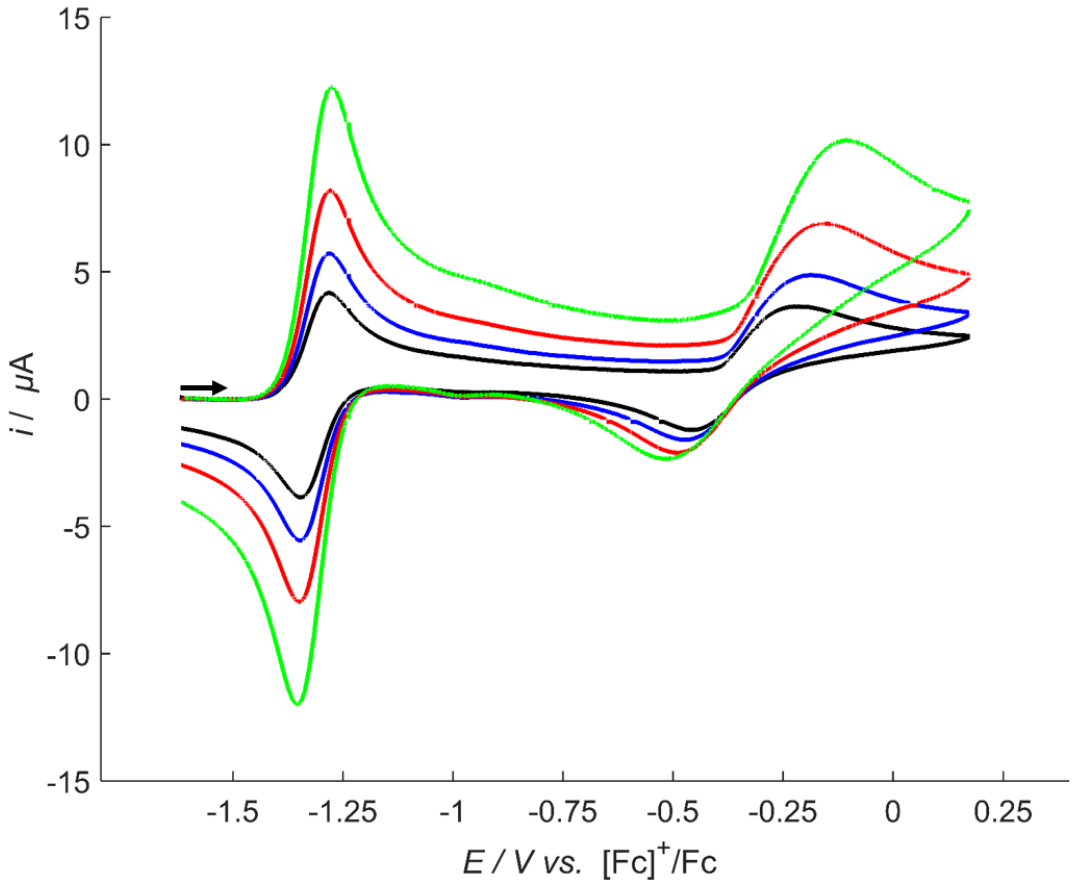

Figure S31. Experimental CV current-potential curves of 0.3 mM $Ni(PMe_3)_4$ in 0.1 M nBu_4NPF_6/ 1,2-$C_6H_4F_2$, T = 24°C at different scan rates: ν = 50 (black), 100 (blue), 200 (red), and 500 mV s^{-1} (green); initial scan direction is indicated by black arrow.

	E^0/mV vs Fc/$[Fc]^+$	**ΔE/ mV**	**i_p(red)/i_p(ox)**
$[Ni(PMe_3)_4]^{0/+}$	–1311	69 ± 5	1.039 ± 0.006 [a]
$[Ni(PMe_3)_4]^{+/2+}$	–332	282 ± 57	variable [b]

[a] i_p(red)/i_p(ox) independent of potential sweep rate and concentration.

[b] i_p(red)/i_p(ox) averaged over three concentrations (0.1, 0.2, and 0.3 mM); 50 mV s^{-1}: 1.261 ± 0.023; 100 mV s^{-1}: 1.257 ± 0.008; 200 mV s^{-1}: 1.299 ± 0.065; 500 mV s^{-1}: 1.119 ± 0.008.

7. Additional Details on Product Mixture from [1]NTf$_2$ and Na[HB(OAc)$_3$]

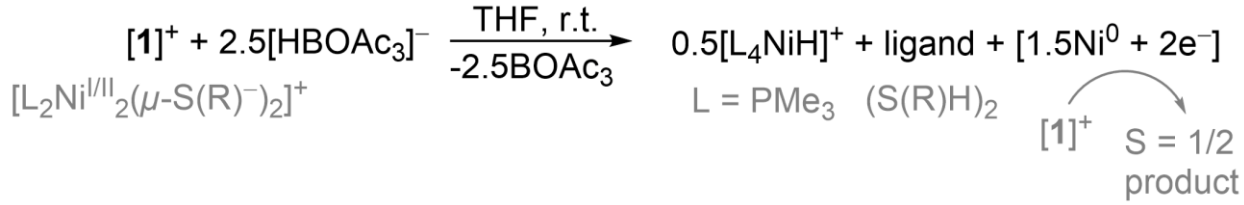

A suspension of sodium tris(acetoxy)borohydride (5.0 mg, 0.023 mmol) in 0.25 mL of d_8-THF was added dropwise to a solution of [**1**]NTf$_2$ (27.0 mg, 0.022 mmol) in 0.25 mL d_8-THF, and the mixture stirred for 0.5 h at r.t. Over this time, the colour changed from dark brown to red brown. The reaction mixture was filtered and product composition analyzed by ^{1}H NMR spectroscopy using 1,3,5-(MeO)$_3$C$_6$H$_3$ as internal standard; cf. Figures S32-33.

Quantitative analysis by NMR spectroscopy corroborated the formation of 10 % of [HNi(PMe$_3$)$_4$]$^+$, 20 % of 1,4-terphenyldithiophenol ligand, and ≤ 80 % of a paramagnetic complex, cf. Figure S32. X-band cw-EPR spectra were acquired from a 2-Me-thf glass at 110 K and corroborated full conversion of [**1**]$^+$ and the formation of a distinct S = 1/2 co-product as shown in Figure S33. Spectra are of rhombic appearance. Principal g-values and hyperfine coupling (hfc) by two distinct ^{31}P rule out the formation of **1**-H. The latter results from nucleophilic attack of hydride at the central π-system of [**1**]$^+$. X-band cw-EPR data of the latter were obtained from a sample of **1**-H that was prepared independently starting from [**1**-H]$^+$ and Cp$_2$Co in 2-Me-THF solution at 24°C. Calculation of principal g-values and hfc constants from rhombic data indicates magnetically equivalent ^{31}P nuclei (A_{iso}(^{31}P) ≈ 255 MHz) for **1**-H; cf. Figure S 34-35. Taken together, treatment of [**1**]$^+$ (= Ni^{I}/ Ni^{II}) with 2.5 equiv. of H$^-$ (= 2.5 H$^+$/ 5e$^-$) affords 0.5 [HNi(PMe$_3$)$_4$]$^+$ (= Ni^0 + H$^+$) and free ligand (2H$^+$). It is assumed that remaining Ni$^{2+/+}$ converts ≈ 80 % of unreacted starting material [**1**]$^+$ into paramagnetic co-product.

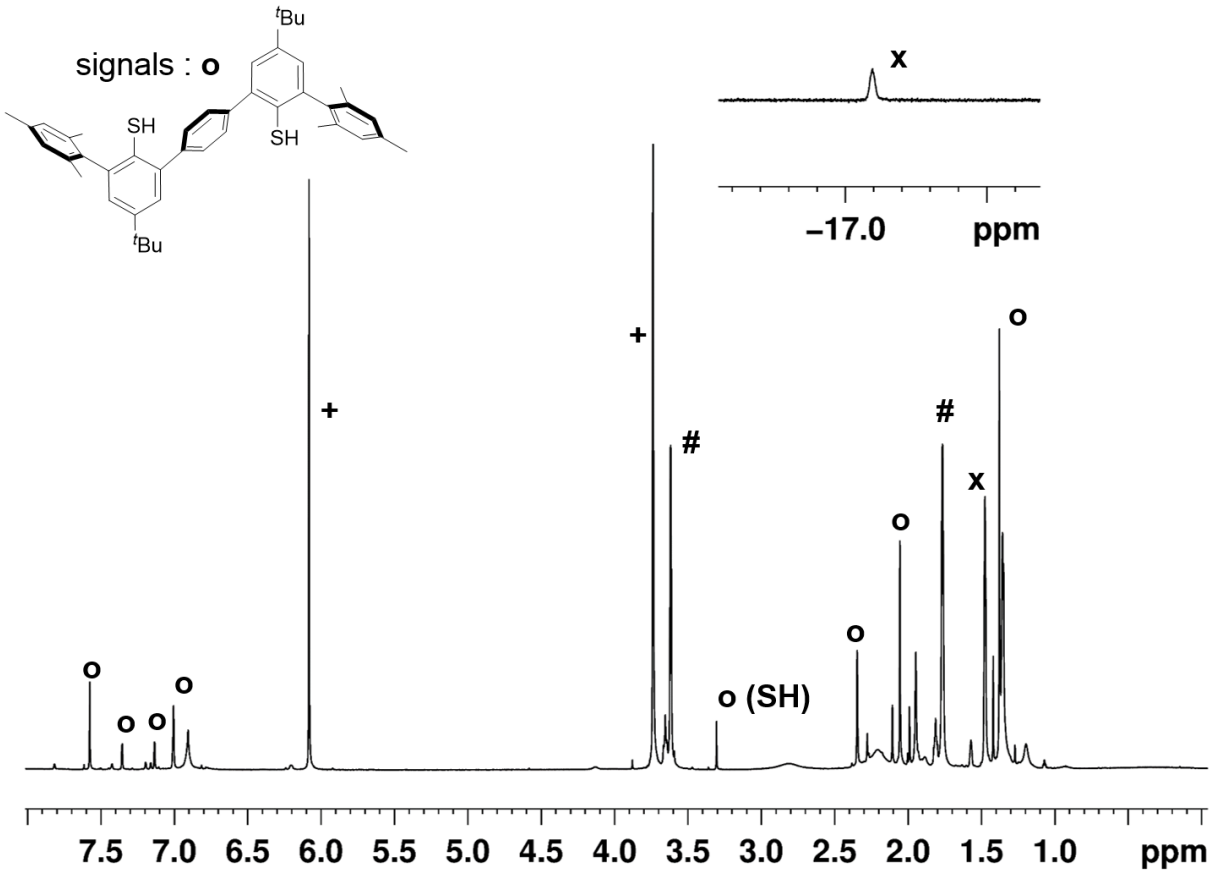

Figure S32. ^{1}H NMR spectrum (500 MHz, d_8-THF (#), 26°C): Products from treatment of [**2**]$^{2+}$ with 1 equiv. of $[HB(OAc)_3]^-$; 1,3,5-trimethoxybenzene (+, internal standard); *Bottom*, characteristic resonances of free dithiophenol ligand (**O**, *e.g.* SH at 3.3 ppm)[6] and $[HNi(PMe_3)_4]^+$ (**X**); *Right inset*: magnification of high field region showing the Ni-H resonance of $[HNi(PMe_3)_4]^+$.

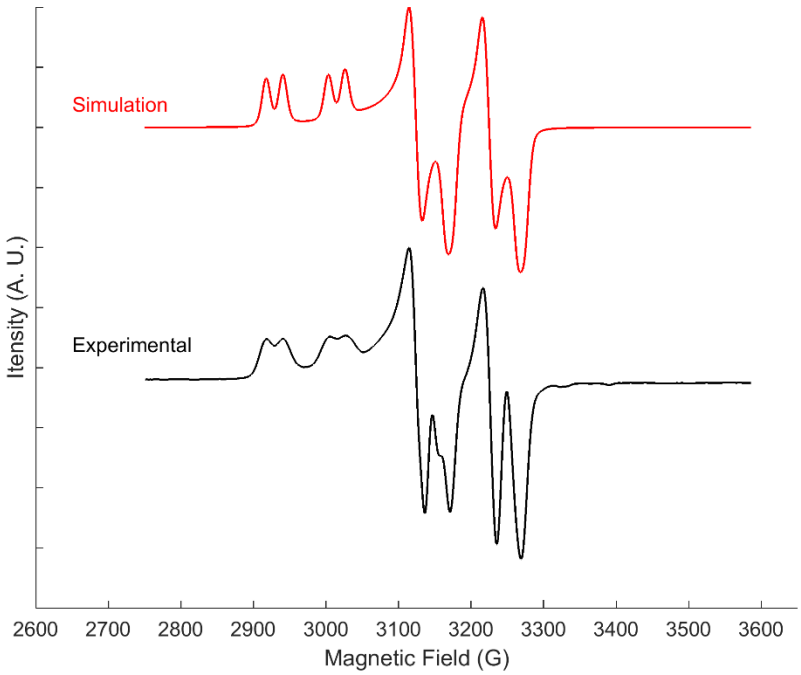

Figure S33. Digitally simulated (red) and experimental (black, 1:1 2-Me-THF/THF glass, 110 K) X-band cw-EPR spectra of a mixture of $[\mathbf{1}]^{+}$ and $[HB(OAc)_3]^{-}$. Microwave frequency 9.30561 GHz, microwave power 2.00 mW, modulation amplitude 2 G. Simulated parameters: $g_x = 2.24$; $g_y = 2.09$; $g_z = 2.06$; $A_{x1} = 267$; $A_{y1} = 296$; $A_{z1} = 2285$; $A_{x2} = 72$; $A_{y2} = 20$; $A_{z2} = 28$ MHz, full line width at half maximum: 1.13 (Gaussian); 0.38 (Laurentzian).

A solution of Cp_2Co (46 mg, 0.1 mM in C_6D_6) was added dropwise to a solution of [**1-H**]NTf_2 (5 mg, 0.0042 mmol) in 2-Me-THF (2mL) at r.t. The solution was filtered to remove sparingly soluble $[Cp_2Co]NTf_2$ co-product and an X-band cw-EPR spectrum was recorded at 110 K.

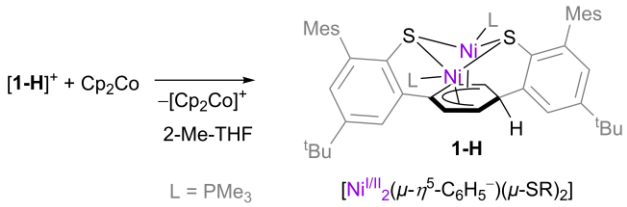

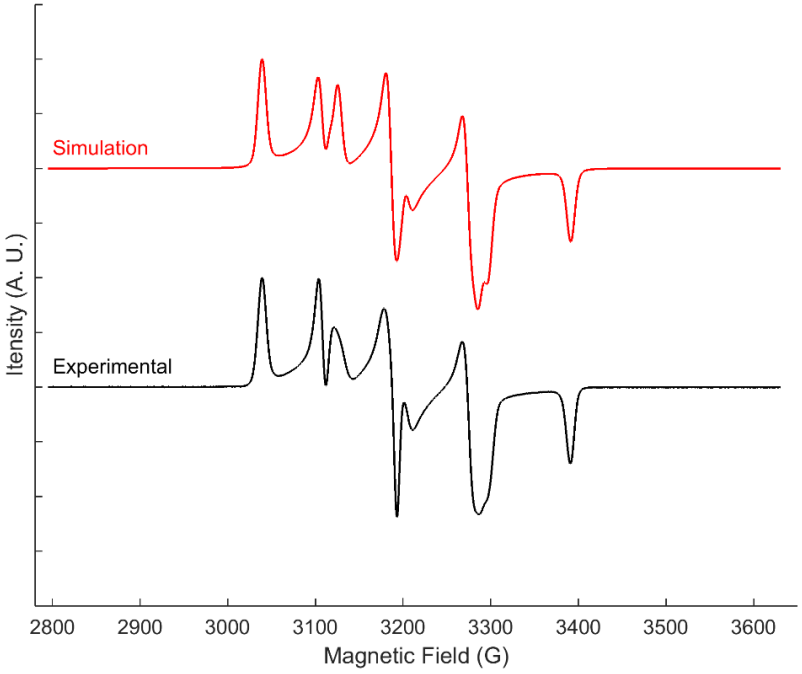

Figure S34. Digitally simulated (red) and experimental (black, 2-Me-THF glass, 110 K) X-band cw-EPR spectra of **1**-H generated in situ from [**1**-H]$^+$ and Cp_2Co. Microwave frequency 9.304729 GHz, microwave power 2.00 mW, modulation amplitude 2 G. Simulated parameters: $g_x = 2.13$; $g_y = 2.08$; $g_z = 2.02$; $A_{x1} = 226$; $A_{y1} = 227$; $A_{z1} = 266$; $A_{x2} = 257$; $A_{y2} = 254$; $A_{z2} = 296$ MHz, full line width at half maximum: 0.935 (Gaussian); 0.29 (Laurentzian).

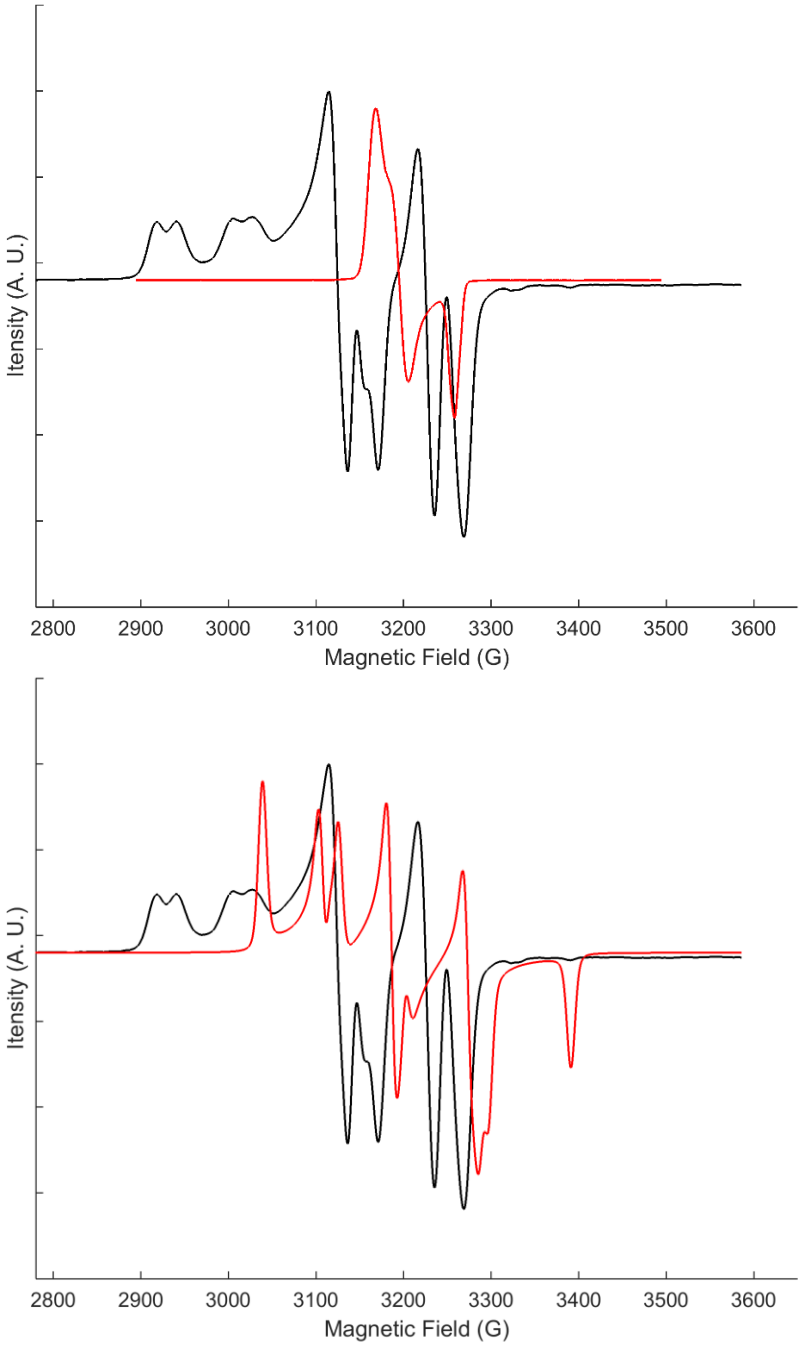

Figure S35. Superposition of X-band cw-EPR spectra of reaction mixture of $[\mathbf{1}]^+$ and $[HB(OAc)_3]^-$ (black, cf. Figure S33) and starting material $[\mathbf{1}]^+$ (red, *top*)[1] and **1**-H (red, *bottom*).

8. References

F. Koch, A. Berkefeld, H. Schubert and C. Grauer, *Chem. Eur. J.*, 2016, **22**, 14640-14647.
F. Koch, A. Berkefeld, B. Speiser and H. Schubert, *Chem. Eur. J.*, 2017, **23**, 16681-16690.
D. J. Krysan and P. B. Mackenzie, *J. Org. Chem.*, 1990, **55**, 4229-4230.
C. A. Tolman, *J. Am. Chem. Soc.*, 1970, **92**, 2956-2965.
S. Stoll and A. Schweiger, *J. Magn. Res.*, 2006, **178**, 42-55.
F. Koch, H. Schubert, P. Sirsch and A. Berkefeld, *Dalton Trans.*, 2015, **44**, 13315-13324.